iScience

CellPress

Article

Large-Scale Analysis of the Diversity and Complexity of the Adult Spinal Cord Neurotransmitter Typology

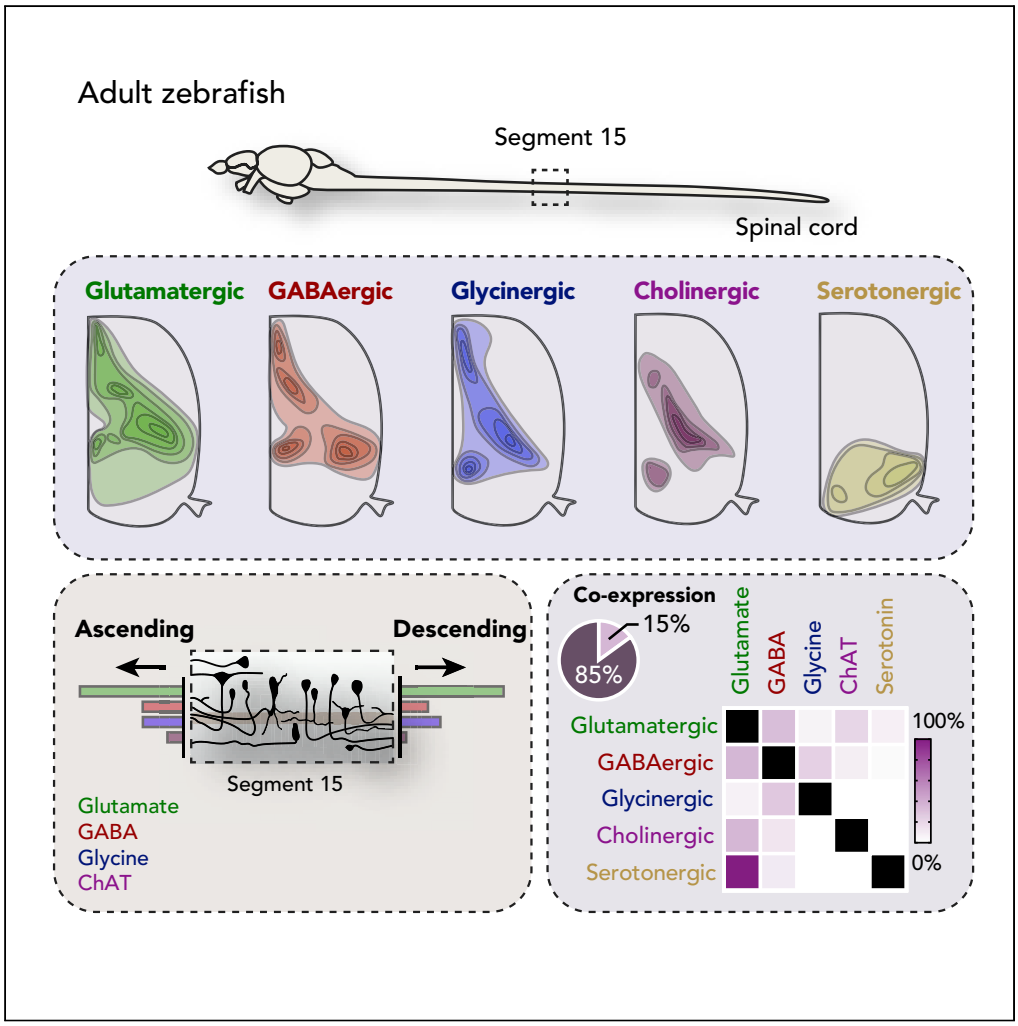

Andrea Pedroni, Konstantinos Ampatzis

konstantinos.ampatzis@ki.se

HIGHLIGHTS

The structural organization of the adult zebrafish spinal cord is highly diverse

Equal number of ascending and descending neurons are excitatory or inhibitory

Several (~15%) spinal neurons express multiple neurotransmitter phenotypes

Part of the glutamatergic V2a-INs co-express GABA, glycine, or acetylcholine

Pedroni & Ampatzis, iScience *19*, 1189–1201
September 27, 2019
https://doi.org/10.1016/j.isci.2019.09.010

iScience

CellPress

Article

Large-Scale Analysis of the Diversity and Complexity of the Adult Spinal Cord Neurotransmitter Typology

Andrea Pedroni[1] and Konstantinos Ampatzis[1,2,*]

SUMMARY

The development of nervous system atlases is a fundamental pursuit in neuroscience, since they constitute a fundamental tool to improve our understanding of the nervous system and behavior. As such, neurotransmitter maps are valuable resources to decipher the nervous system organization and functionality. We present here the first comprehensive quantitative map of neurons found in the adult zebrafish spinal cord. Our study overlays detailed information regarding the anatomical positions, sizes, neurotransmitter phenotypes, and the projection patterns of the spinal neurons. We also show that neurotransmitter co-expression is much more extensive than previously assumed, suggesting that spinal networks are more complex than first recognized. As a first direct application, we investigated the neurotransmitter diversity in the putative glutamatergic spinal V2a-interneuron assembly. These studies shed new light on the diverse and complex functions of this important interneuron class in the neuronal interplay governing the precise operation of the central pattern generators.

INTRODUCTION

Neuronal networks in the spinal cord are able and sufficient to generate and control movements and receive and process sensory information (Arber, 2012; Goulding, 2009; Grillner and Jessell, 2009; Kiehn, 2016). Their functionality depends on the correct specification of different classes of neurons during development (Alaynick et al., 2011; Arber, 2012; Goulding, 2009; Jessell, 2000), which allows them to establish precise connections. Spinal neurons derive from specific progenitor pools in the spinal cord and express precisely a combination of transcription factors (Alaynick et al., 2011; Arber, 2012; Goulding, 2009; Jessell, 2000). Their developmental diversification is well understood (Arber, 2012; Goulding, 2009; Jessell, 2000; Kiehn, 2016), but it is not clear how several functional characteristics of these cells are specified. A particularly important determinant of a neuron's functionality is its neurotransmitter phenotype.

Neuronal communication involves the release and uptake of specific neurotransmitters (Rogawski and Barker, 1986; Schwartz, 2000), endogenous chemical messengers used in intercellular signaling across synapses. The vertebrate nervous system uses neurotransmitters including glutamate, γ-aminobutyric acid (GABA), glycine, and acetylcholine to mediate biological functions such as sensory perception and to generate complex behaviors (Rogawski and Barker, 1986; Schwartz, 2000; Unwin, 1993). Neurons can be classified as excitatory, inhibitory, or modulatory based on their neurotransmitter phenotypes. Therefore, the adoption of a specific neurotransmitter system by a given neuron type defines its identity. To understand specific neurons' roles in integrated neural networks, one must identify the transmitters they use to modulate their targets. Neuroanatomically precise maps of neurotransmitter typology distributions facilitate this by revealing correlations between the anatomical and functional neuronal architectures.

The zebrafish is an important model organism for high-throughput studies on neuronal circuits' functions and behavior, and much is known about the different cell types in the zebrafish spinal cord (Ampatzis et al., 2013; Bernhardt et al., 1990, 1992; Björnfors and El Manira, 2016; Bradley et al., 2010; Böhm et al., 2016; Djenoune et al., 2017; Hale et al., 2001; Higashijima et al., 2004a, 2004b; Kimura et al., 2008; Liao and Fetcho, 2008; McLean et al., 2007; Menelaou et al., 2014; Satou et al., 2012; Stil and Drapeau, 2016). However, the number and identity of the spinal excitatory and inhibitory neurons that process sensory-related information are unknown, as are the neurotransmitter identities of the neurons that control and gate motor commands. This is a critical limitation because neuronal activity depends strongly on neurotransmitter identity. To overcome this limitation, we conducted the first systematic quantitative neurotransmitter

[1]Karolinska Institutet, Department of Neuroscience, 171 77 Stockholm, Sweden

[2]Lead Contact

*Correspondence: konstantinos.ampatzis@ki.se

https://doi.org/10.1016/j.isci.2019.09.010

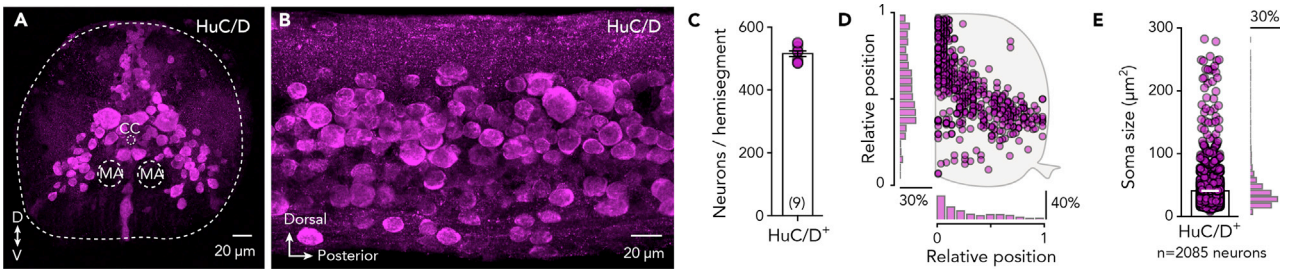

Figure 1. Neuroanatomy of Adult Zebrafish Spinal Cord

(A and B) Transverse section and whole-mount adult zebrafish spinal cord showing the expression of the pan-neuronal marker HuC/D$^+$ neurons.

(C) Quantification of the number of spinal neurons (HuC/D$^+$) located in adult spinal cord hemisegment (segment 15).

(D) Spatial distribution of the HuC/D$^+$ neurons with the medio-lateral and dorsoventral density plot from one adult zebrafish spinal hemisegment (n = 478 labeled cells).

(E) Quantification and distribution of the HuC/D$^+$ neurons soma size (n = 2,085 neurons).

Data are presented as mean ± SEM. CC, central canal; MA, Mauthner axon. For antibodies information, see also Table S1.

phenotype analysis of neurons in adult zebrafish spinal networks by using an anatomical high-throughput strategy to investigate individual populations of spinal excitatory, inhibitory, and modulatory neurons. Our results reveal a previously unsuspected co-expression of different neurotransmitters in spinal cord neurons, and we show that these multi-phenotype neurons are far more numerous and widely distributed in the spinal cord than previously assumed. We use this comprehensive neurotransmitter map to describe the co-existence of classical neurotransmitters in the presumed putative glutamatergic V2a interneuron population, revealing an unsuspected neurotransmitter co-expression within this cohered group of interneurons. The comprehensive neurotransmitter typology atlas presented here reveals an unforeseen diversity, complexity, and dynamics in the principles that govern the structural organization of the adult zebrafish spinal cord and provides an anatomical framework to guide further functional dissection of spinal neuronal circuits.

RESULTS

Neuronal Composition of the Adult Spinal Cord

We first sought to determine the number of neurons in a representative hemisegment (segment 15) of the adult zebrafish spinal cord by using immunohistochemistry to detect the expression of the pan-neuronal marker HuC/D. This revealed that neurons were distributed throughout the adult spinal cord, from the most dorsal and medial part to the most lateral aspects (Figures 1A, 1B, and 1D). However, only a small fraction of the labeled neurons was observed in the ventral part of the spinal hemisegment and the dorsal neuropil area (Figure 1D). Detailed quantification showed that an adult zebrafish spinal hemisegment contains 515.7 ± 8.865 neurons (segment 15; Figure 1C). Although the soma sizes of the labeled spinal neurons varied considerably, the vast majority were small or medium sized (41.17 ± 0.63 µm^2, n = 2085 neurons; Figure 1E). These results show that the adult spinal cord has a well-defined and diverse neuron population and provides a starting point for further characterizing the neurochemical architecture of adult zebrafish spinal cord networks.

Neurotransmitter Typology of Spinal Cord Neurons

Despite previous studies on zebrafish spinal neurotransmitter phenotypes (Higashijima et al., 2004a, 2004b), the number, size, and location of the neurons involved in the spinal networks are currently unknown. Therefore, to provide a reliable foundation for computational modeling and to identify new targets for electrophysiological recordings, we attempted to create a complete and detailed map of the neurotransmitter typology in the adult zebrafish spinal cord. All spinal neurons were found to express one of the classical neurotransmitters considered in this work (glutamate, GABA, glycine, acetylcholine, and serotonin; Figures 2A–2D). In keeping with previous reports, we detected no dopaminergic or noradrenergic spinal neurons (McLean and Fetcho, 2004; Figure S1). The glutamatergic, GABAergic, and glycinergic neurons had similar distributions (Figures 2A–2C), whereas cholinergic neurons were almost absent from the dorsal part of the spinal cord (Figure 2D) and serotonergic neurons were observed only in the ventral part (Figure 2E). Quantification of individual neuronal classes revealed that most neurons are glutamatergic (212.1 ± 5.01 neurons, n = 9 zebrafish), GABAergic (145.5 ± 2.918 neurons, n = 10 zebrafish),

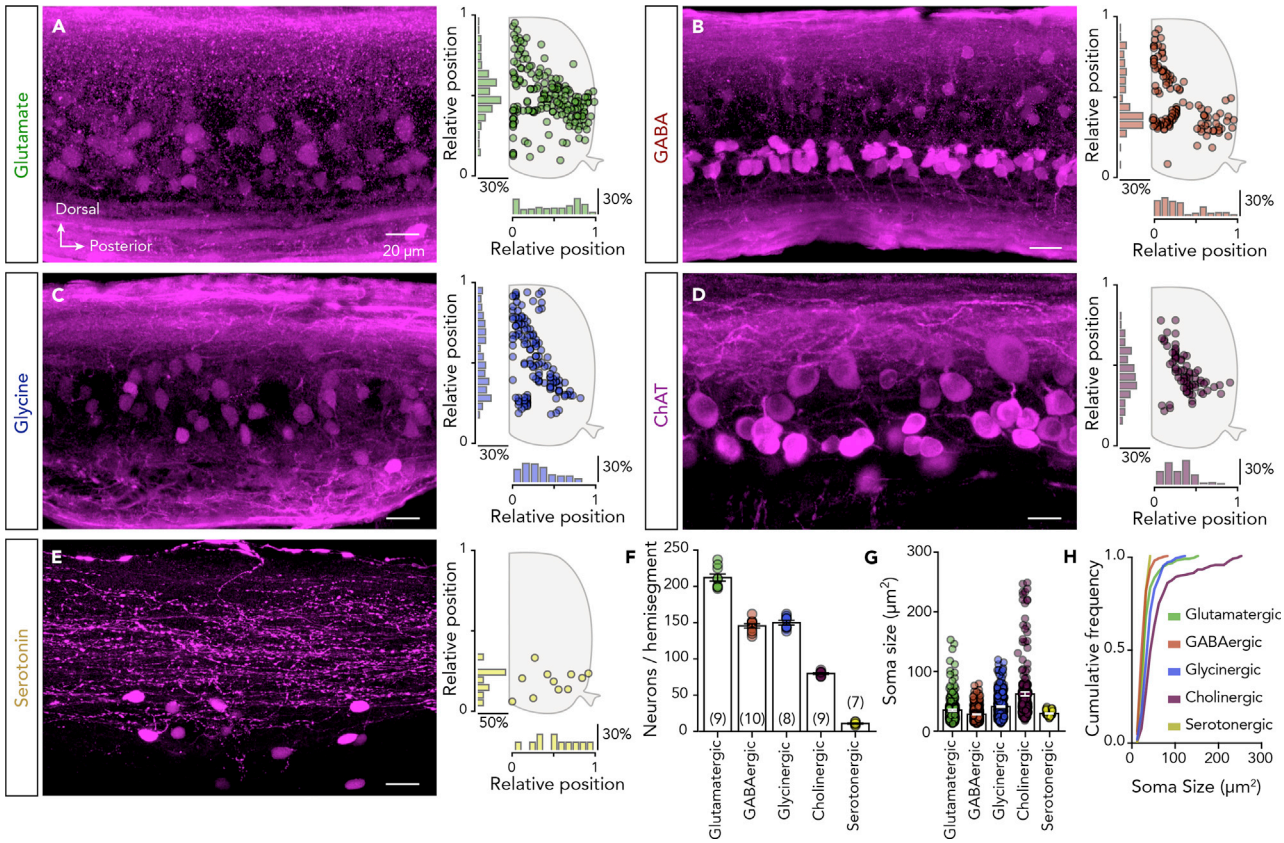

Figure 2. Neurotransmitter Phenotypes of the Adult Zebrafish Spinal Neurons

(A–E) Representative whole-mount photomicrographs showing part of the immunolabeled cells for glutamate, GABA, glycine, ChAT, and serotonin, followed by a schematic representation of the spatial distribution with the corresponding medio-lateral and dorsoventral density plots from a single adult zebrafish spinal cord hemisegment.

(F) Quantification of the total number of the labeled neurons expressing a specific neurotransmitter phenotype.

(G and H) Quantification and cumulative frequency of labeled neurons soma size.

Data are presented as mean ± SEM. For related data and antibodies information, see also Figures S1 and S5 and Table S1.

and glycinergic (150 ± 3.179 neurons, n = 8 zebrafish; Figure 2F). Cholinergic neurons constitute a smaller population (79.78 ± 1.024 neurons, n = 9 zebrafish), and only few serotonergic neurons were found (11 ± 0.755 neurons, n = 7 zebrafish; Figure 2F). Finally, soma size measurements showed that all these neuronal populations had similar mean soma sizes; however, the cholinergic and serotonergic neurons displayed the greatest and least soma size variability, respectively (glutamatergic: 35.11 ± 1.57 µm^2, n = 206 neurons; GABAergic: 27.99 ± 0.525 µm^2, n = 407 neurons; glycinergic: 41.04 ± 0.953 µm^2, n = 379 neurons; cholinergic: 62.54 ± 3.427 µm^2, n = 208 neurons; serotonergic: 29.5 ± 0.815 µm^2, n = 37 neurons; Figures 2G and 2H). The distributions of the different neurotransmitter-expressing neurons in the adult zebrafish spinal cord are thus highly stereotypic and heterogeneous.

Neurotransmitter Phenotypes of Projecting Spinal Neurons

The projection patterns of the spinal cord neurons must be understood to explain their inputs to the circuits that process sensory information and control motor behaviors. We therefore used an anatomical tracing technique to determine the positions, number, and sizes of the projecting spinal neurons. Specifically, we identified every neuron located in hemisegment 15 that projects over five or more spinal segments to a rostral (ascending) or caudal (descending) spinal cord (Figures 3A and 3B). We found that most ascending neurons (~75%) are located in the dorsal and medial part of the spinal cord, whereas the descending neurons are located in the motor column area (Figures 3C and 3D). Furthermore, the ascending neurons comprise a significantly smaller population (71.29 ± 2.212 neurons) than the descending neurons (87.38 ± 2.639 neurons; unpaired t test: t = 4.594, df = 13, P = 0.0005; Figure 3E), and their soma sizes differ

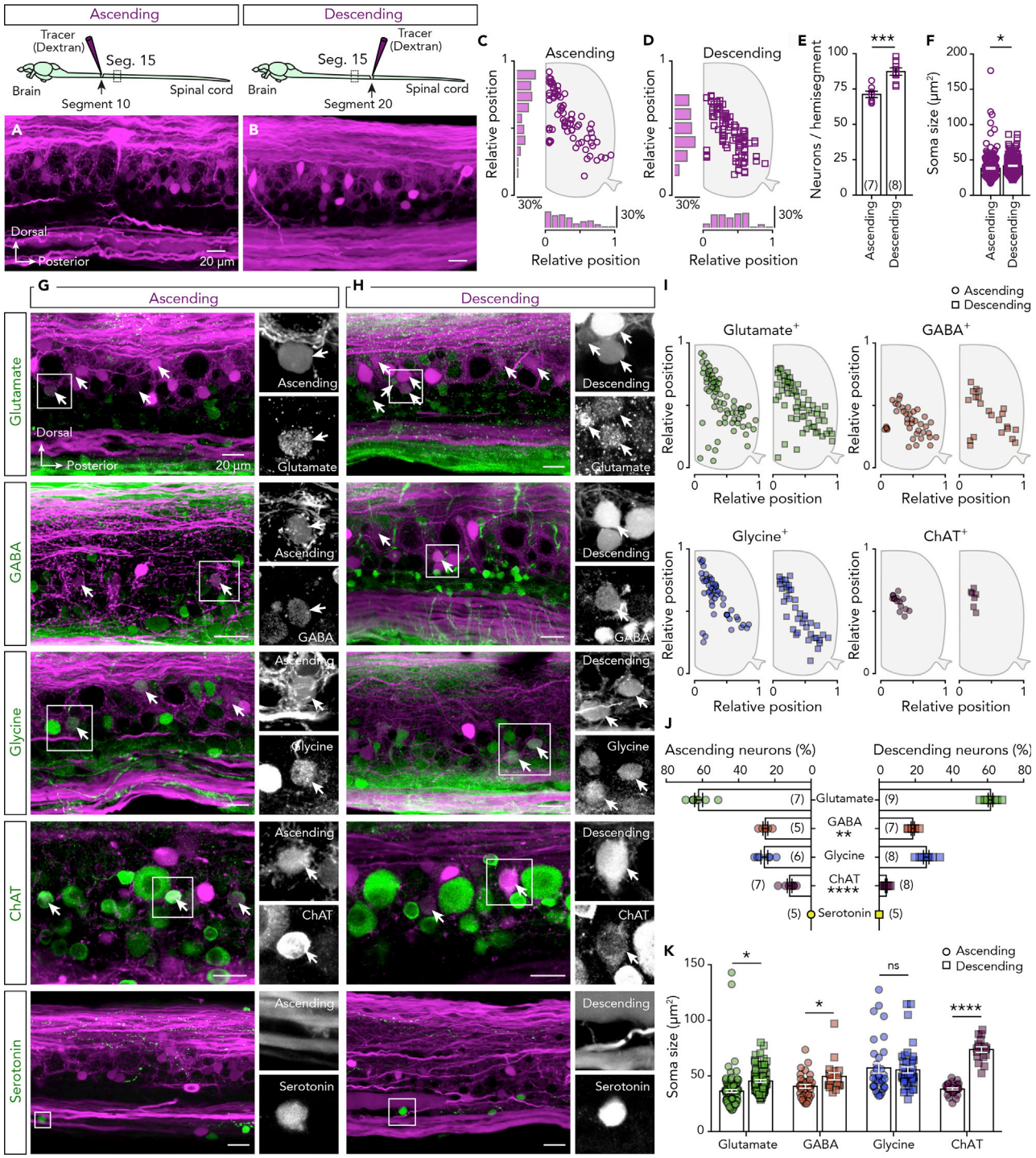

Figure 3. Neurotransmitter Phenotype of Projecting Neurons

(A and B) Injection of a dextran tracer in segment 10 or 20 reveals the ascending and descending spinal projecting neurons, respectively, located in spinal cord segment 15.

(C and D) Setting positions of the tracer-labeled ascending (circles) and descending (squares) neurons that project to the rostral or caudal part of the spinal cord revealed in one representative preparation.

(E) Quantification of the total number of ascending and descending neurons detected in the spinal cord hemisegment.

(F) Plot showing the soma sizes of the tracer-labeled ascending and descending neurons (Ascending: n = 217 neurons; Descending: n = 185 neurons).

Figure 3. *Continued*

(G and H) Double staining between ascending or descending traced neurons (magenta) with glutamate, GABA, glycine, ChAT, and serotonin (green). Arrows indicate the double-labeled neurons. On the right side, there are single channel magnifications of the boxed area.

(I) Spatial distribution of the ascending (circles) and descending (squares) traced neurons that express a specific neurotransmitter phenotype.

(J) Quantification of percentage of tracer-positive ascending and descending projecting neurons expressing each neurotransmitter phenotype.

(K) Soma sizes of the tracer-positive ascending (circles) and descending (squares) projecting neurons.

Data are presented as mean ± SEM; *P < 0.05; **P < 0.01; ***P < 0.001; ****P < 0.0001; ns, non-significant. For antibodies information, see also Table S1.

(ascending: 38.33 ± 1.106 μm^2, *n* = 217 neurons; descending: 41.76 ± 0.894 μm^2, *n* = 185 neurons; unpaired t test: t = 2.354, df = 400, P = 0.0191; Figure 3F).

To determine the projecting neurons' neurotransmitter phenotypes, we combined the tracing with immunolabeling of the classical neurotransmitters (Figures 3G and 3H). This revealed that the ascending neurons located in the most dorsal area of the spinal cord are glutamatergic and glycinergic (Figure 3I), whereas GABAergic and cholinergic projecting neurons are co-distributed in the medial and ventral parts of the spinal cord (Figure 3I). In addition, no serotonergic neurons displayed ascending or descending projections extending over more than five segments (Figures 3G and 3H). Quantitative transmitter phenotype analyses showed that most projecting neurons are glutamatergic (ascending: 62.12 ± 2.2%, n = 7 zebrafish; descending: 61.67 ± 1.3%, *n* = 9 zebrafish; Figure 3J), whereas GABAergic (ascending: 25.29 ± 1.323%, *n* = 5 zebrafish; descending: 18.6 ± 0.858%, *n* = 7 zebrafish) and glycinergic (ascending: 25.87 ± 1.899%, *n* = 6 zebrafish; descending: 26.09 ± 1.542%, *n* = 8 zebrafish) neurons form notably smaller populations. We also found a few projecting cholinergic neurons (ascending: 11.87 ± 1.297%, *n* = 7 zebrafish; descending: 3.96 ± 0.506%, *n* = 8 zebrafish; Figure 3J). With GABAergic (unpaired t test: t = 4.45, df = 10, P = 0.0012; Figure 3J) and cholinergic (unpaired t test: t = 5.975, df = 13, P < 0.0001; Figure 3J) projecting neurons to exhibit significant differences. Our analysis suggests that similar patterns of excitation and inhibition are delivered to the rostral and caudal parts of the spinal cord. Finally, to determine whether different neuron types innervate the rostral and caudal parts of the spinal cord, we quantified the soma sizes of projecting neurons with respect to their neurotransmitter phenotypes (Figure 3K). Although in most cases the soma sizes of the ascending and descending neurons were significantly different (unpaired t test: glutamatergic: t = 2.33, df = 143, P = 0.021; GABAergic: t = 2.652, df = 52, P = 0.01; Figure 3K), only the cholinergic neurons displayed populations with non-overlapping sizes (unpaired t test: t = 15.22, df = 43, P < 0.0001; Figure 3K), suggesting that they constitute two distinct projecting subpopulations.

Spinal Neurons Express Multiple Neurotransmitter Phenotypes

Our analysis of neurotransmitter phenotypes in adult zebrafish spinal neurons suggested that the total number of neurons expressing a specific classical neurotransmitter is ~600. Since we detected 515 neurons in each spinal cord hemisegment, this possibly implies that some spinal cord neurons (~15%) express multiple neurotransmitter phenotypes. To test this hypothesis, the extent of co-expression was determined using binary neurotransmitter immunodetection. We found that several neurons co-express two neurotransmitter phenotypes (Figure 4A) and that these neurons have specific distribution patterns in the spinal cord (Figure 4C). However, we found no co-expression of ChAT with serotonin and glycine or of glycine with serotonin (Figure 4A). To determine whether neurons with dual neurotransmitter phenotypes comprise separate neuronal subpopulations that settle at distinct positions in the spinal cord, we measured the somas of double-labeled neurons (Figure 4B).

Next, we determined the extent of dual neurotransmitter expression in different neuron populations. We found that a notable proportion of glutamatergic neurons are GABAergic (19.46 ± 1.302%, *n* = 12 zebrafish), cholinergic (16.37 ± 0.927%, *n* = 9 zebrafish), serotonergic (4.814 ± 0.224%, *n* = 8 zebrafish), or glycinergic (4.507 ± 0.758%, *n* = 6 zebrafish; Figure 4D). In addition, many GABAergic neurons co-express glutamate (27.76 ± 1.879%, *n* = 12 zebrafish) or glycine (19.2 ± 1.922%, *n* = 6 zebrafish), and a few were immunolabeled for choline acetyltransferase (ChAT; 6.965 ± 0.602%, *n* = 5 zebrafish) or serotonin (0.413 ± 0.185%, *n* = 12 zebrafish; Figure 4E). However, glycinergic neurons were observed to co-express only GABA (18.67 ± 2.057%, *n* = 6 zebrafish) and glutamate (6.008 ± 0.9372%, *n* = 6 zebrafish; Figure 4F), as do cholinergic neurons (GABA: 12.62 ± 1.15%, *n* = 5 zebrafish; Glutamate: 42.42 ± 2.311%, *n* = 9 zebrafish; Figure 4G). Finally, many serotonergic neurons were found glutamatergic (93.19 ± 2.83%, *n* = 8 zebrafish), and a few occasionally (4 of 12 zebrafish) to co-express GABA (5.623 ± 2.47%, *n* = 12 zebrafish; Figure 4H). Most notably, the GABAergic/serotonergic neurons were found to consist of a subpopulation of the

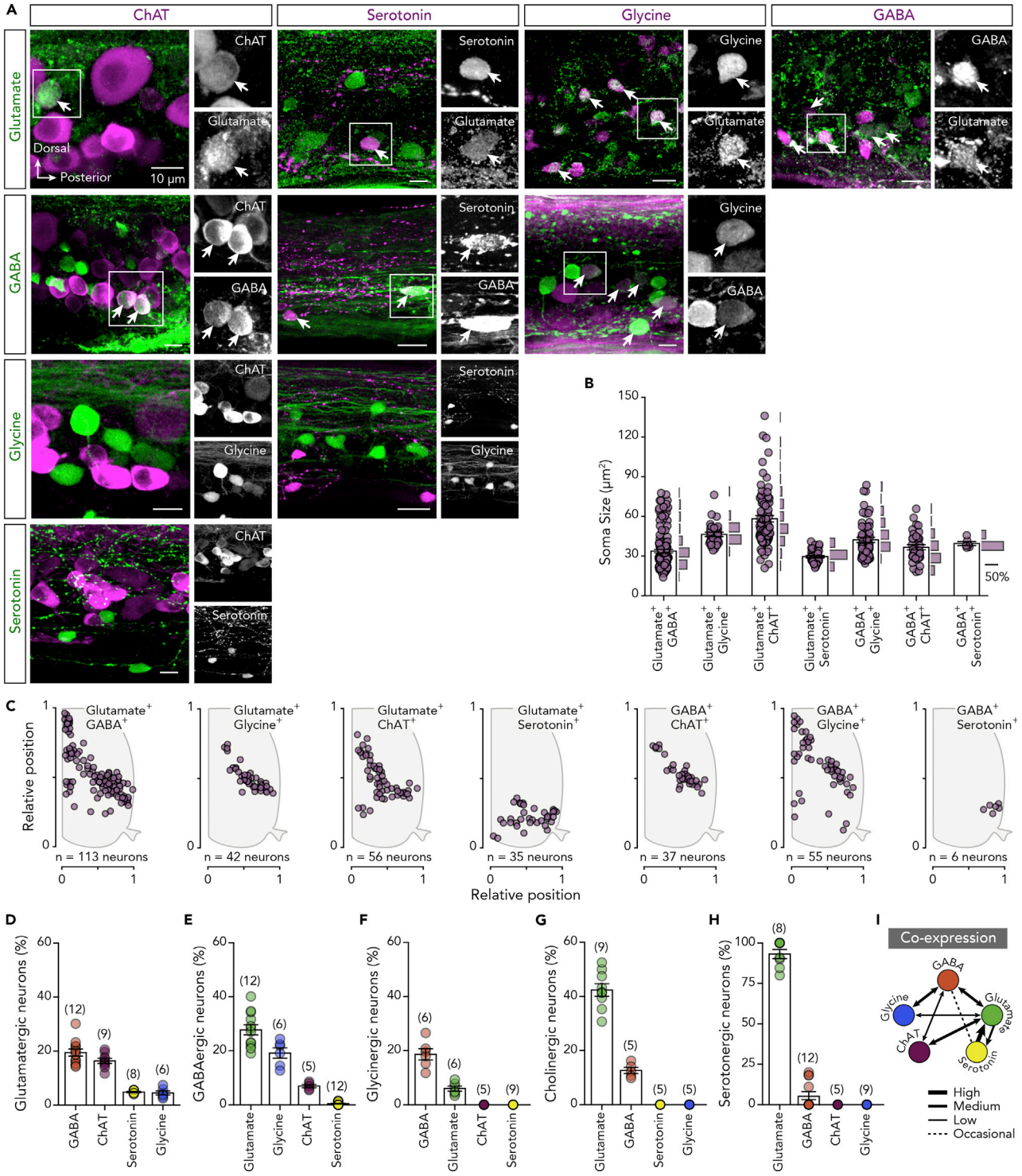

Figure 4. Spinal Cord Neurons Express Multiple Neurotransmitter Phenotypes

(A) Whole-mount double immunolabeling between glutamate, GABA, glycine, ChAT, and serotonin. In black and white are single channel images of the merged images. Arrows indicate the double-labeled neurons.

(B and C) Soma sizes and spatial distribution of the detected double-stained neurons in the adult zebrafish spinal cord hemisegment.

Figure 4. *Continued*

(D–H) Quantification of percentage of glutamatergic, GABAergic, glycinergic, cholinergic ($ChAT^+$), and serotonergic neurons that co-express other neurotransmitters.

(I) Schematic relationship of the neurotransmitters co-expression from the adult zebrafish spinal cord neurons.

Data are presented as mean ± SEM. For related data and antibodies information, see also Figures S2 and S3 and Table S1.

serotonergic neurons that possess larger soma sizes (Figure 4B) and their distribution is restricted to the ventral and lateral part of the spinal cord (Figure 4C).

The validity of our observations was confirmed also by immunohistochemistry using transgenic animal lines (*VGlut2a:GFP; GAD1b:GFP; GlyT2:GFP* and *Tph2:GFP*) to detect the proposed neurotransmitter phenotypes (see Transparent Methods, Figures S2 and S5). To verify that spinal neurons can co-release different neurotransmitters, we performed *in situ* hybridization experiments using the sensitive RNAscope method to detect individual mRNAs for the vesicular glutamate transporter (VGlut2a, *slc17a6b*) found in neurons that release glutamate as a transmitter (Shigeri et al., 2004), the vesicular acetylcholine transporter (vAChT, *slc18a3b*; a specific transporter of cholinergic neurons, Weihe et al., 1996), and the vesicular GABA transporter (vGAT, *slc32a1*; also known as vIAAT, vesicular inhibitory amino acid transporter) a transporter for both GABAergic and glycinergic neurons (Chaudhry et al., 1998; Wojcik et al., 2006, Figures S3A–S3C). We observed the presence of different combinations (co-localizations) of the vesicular transporter mRNA puncta in individual neurons (Figures S3D–S3G), confirming that adult spinal cord neurons host the cellular machinery needed to store and release (co-transmit) different classical neurotransmitters. Interestingly, we also observed small populations of spinal neurons containing all three vesicular transporter mRNA puncta (Figure S3G), suggesting the existence of triple co-transmission. We verified this observation by immunohistochemistry and investigated the distribution and soma sizes of spinal cholinergic neurons that co-express GABA and glutamate (Figure S3H).

Together, these data provide the first evidence that the characterization of neurons as being either excitatory or inhibitory is an oversimplification that does not properly reflect the neurotransmitter complexity of neuronal populations in the vertebrate spinal cord (Figure 4I).

V2a Interneuron Neurotransmitter Diversity: A Proof-of-Concept Analysis

To evaluate our findings and the extent of neurotransmitter co-expression and dynamics, we performed a proof-of-concept analysis focusing on one of the most well-characterized spinal interneuron populations, the V2a interneurons (Arber, 2012; Goulding, 2009; Kiehn, 2016, 2011). V2a interneurons are one of the most important excitatory neuronal classes for the operation of the vertebrate locomotor network (Al-Mosawie et al., 2007; Crone et al., 2008; Dougherty and Kiehn, 2010; Hayashi et al., 2018; Joshi et al., 2009; Lundfald et al., 2007; Zhong et al., 2011), as demonstrated by studies on zebrafish (Ampatzis et al., 2014; Ausborn et al., 2012; Eklöf-Ljunggren et al., 2012; Kimura et al., 2006; McLean et al., 2008; McLean and Fetcho, 2009; Menelaou et al., 2014; Song et al., 2018). In keeping with previous reports (Ampatzis et al., 2014), we detected 23.59 ± 0.503 V2a interneurons (n = 22 zebrafish; Figure S4B) per hemisegment in the adult zebrafish spinal cord. These interneurons were found to be distributed within the motor column (Figure S4C) and displayed variable soma sizes (Figure S4D). Detailed analysis of the neurotransmitter phenotype of the V2a interneuron population revealed that the vast majority (93.27 ± 1.116%, n = 17 zebrafish; Figures 5A and 5B) were glutamatergic, with occasionally (10 of 14 zebrafish) one and rarely two GFP^+ V2a interneurons appearing as $glutamate^-$. The $glutamate^-$ V2a interneurons had restricted distribution (Figure 5C) and significantly smaller soma (24.61 ± 1.261 μm^2) than those expressing glutamate (48.21 ± 2.902 μm^2; unpaired t test: t = 4.351, df = 104, P < 0.0001, Figure 5D). Interestingly, a smaller fraction of the V2a interneurons appeared to also express GABA (12.31 ± 1.217%, n = 9 zebrafish; Figures 5E and 5I), glycine (10.67 ± 0.84%, n = 7 zebrafish; Figures 5F and 5I), or ChAT (11.9 ± 0.755%, n = 13 zebrafish; Figures 5G and 5I). However, none were found to express serotonin (n = 6 zebrafish; Figures 5H and 5I). Moreover, the $GABA^+$, $glycine^+$, and $ChAT^+$ V2a interneurons had distinct topographic distribution patterns (Figure 5J) and soma sizes (Figures 5K–5N), strongly suggesting that they may constitute different subpopulations of the glutamatergic population. Finally, we sought to determine whether the glutamatergic V2a interneurons could co-transmit these additional neurotransmitters by performing immunohistochemistry and *in situ* hybridization experiments to investigate their ability to produce the vesicular transporters for GABA and glycine (vGAT) and for acetylcholine (vAChT) (Figure S4). We detected vAChT, vGAT, and the glycinergic transporter (GlyT2) in presynaptic terminals ($SV2^+$) of the V2a interneurons (GFP^+, Figure S4E). In addition, vGAT or vAChT mRNAs were detected in a small proportion of the V2a

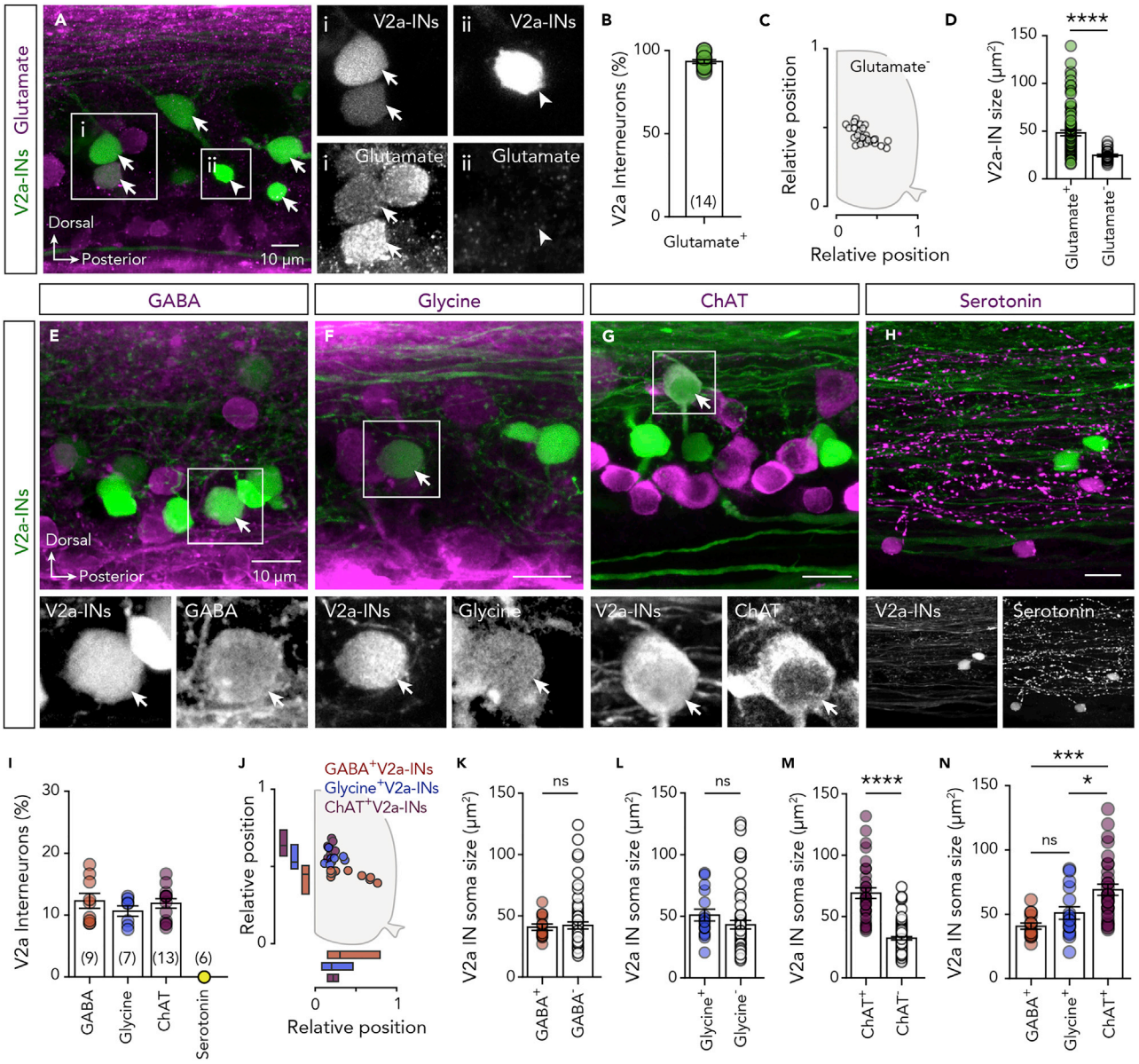

Figure 5. V2a Interneuron Neurotransmitter Diversity

(A and B) Representative whole-mount photomicrographs and analysis showing that the vast majority, but not all, of the adult zebrafish spinal cord V2a interneurons are expressing glutamate. Arrows indicate the double-labeled neurons. Arrowheads indicate the non-glutamatergic V2a interneurons.

(C) Setting positions of the glutamate^{-} (open circles) V2a interneurons in the spinal cord.

(D) Plot showing the difference in soma sizes of the glutamate^{+} (green circles) and glutamate^{-} (open circles) V2a interneurons.

(E-H) Whole-mount double immunolabeling between V2a interneurons with GABA, glycine, ChAT, or serotonin. In black and white are single channel images of the merged images. Arrows indicate the double-labeled neurons.

(I and J) Analysis of the percentage and the topographic organization of the V2a interneurons that express GABA, glycine, or ChAT.

(K–M) Quantification of the V2a interneuron soma sizes that are immune-positive and immune-negative for the GABA, glycine, or ChAT (unpaired t test: t = 10.65, df = 111, P < 0.0001).

(N) Comparison of the V2a interneuron soma sizes that express GABA, glycine, or ChAT (one-way ANOVA: $F_{(2,58)} = 10.44$, P = 0.0001).

Data are presented as mean ± SEM. *P < 0.05; ***P < 0.001; ****P < 0.0001; ns, non-significant. For related data and antibodies information, see also Figure S4 and Table S1.

interneurons by *in situ* hybridization (Figure S4F). These findings confirm our immunohistochemical observations (Figures 5E–5N) and suggest that the V2a interneurons' functional role in the organization and operation of the spinal cord networks controlling animals' movements is more complex than previously recognized.

DISCUSSION

We have conducted the first comprehensive classification of adult zebrafish neurons in a whole spinal cord hemisegment, revealing the total number of neurons, their sizes, the transmitter phenotypes they express, their setting positions, and their projection patterns. We have also established the extent of co-expression of the main classical neurotransmitters in spinal cord neurons, suggesting that the neurons' chemical and anatomical organization is much more complex than previously recognized. Neuronal maps like that presented here, which describe distinct structural and biochemical features, provide essential guidance for future studies on the nervous system's development and function. Cell-type-specific neurotransmitter classifications of spinal neurons will enable further functional analyses of the diverse but stereotypic neuron populations that generate and gate sensory and motor functions to control animal movements.

Signal transmission in neuronal networks involves the release of neurotransmitters that bind specifically to membrane receptors on target neurons to mediate basic and complex biological functions. Since the identity of the neurotransmitters that a neuron synthesizes and releases is an important aspect of its differentiation fate, it is essential to understand the genetic programs that specify an individual neuron's type and transmitter expression. The genetic programs that specify the spinal cord neuronal populations are well defined (Alaynick et al., 2011; Arber, 2012; Goulding, 2009; Jessell, 2000; Kiehn, 2016), but our understanding of neurotransmission within these neuronal classes is limited. Among the neurotransmitters of the nervous system, glutamate, GABA, glycine, acetylcholine, and serotonin are the most well studied in the spinal cords of vertebrates (Alvarez et al., 2005; Antal et al., 1994; Brodin et al., 1990; Mahmood et al., 2009; Phelps et al., 1990; Pombal et al., 2001; Restrepo et al., 2009; Sueiro et al., 2004; Wéber et al., 2007), including zebrafish (Barreiro-Iglesias et al., 2013; Bradley et al., 2010; Böhm et al., 2016; Higashijima et al., 2004a, 2004b; Liao and Fetcho, 2008; McLean and Fetcho, 2004). Several spinal interneuron types have been described in the developing zebrafish spinal cord based on their discrete morphological features (Bernhardt et al., 1990, 1992; Hale et al., 2001), which have been linked to specific neurotransmitter identities (Higashijima et al., 2004a, 2004b). These associations imply that most descending projecting interneurons express glutamate, whereas most ascending projecting neurons express GABA and/or glycine. This reinforces the notion that the principal descending input in the spinal cord is excitatory and the main ascending input is inhibitory. However, our tracing and immunodetection experiments suggest that similar numbers of inhibitory and excitatory neurons project to the rostral and caudal parts of the spinal cord and the vast majority of these neurons are glutamatergic.

Our results firmly establish that many spinal cord neurons (~15%; approximately 80–90 neurons) exhibit multiple neurotransmitter phenotypes. One classical view in neuroscience is that neurons have the ability to produce, store, and release one type of neurotransmitter, a misinterpreted concept of Dale's principle (Eccles et al., 1954), that a neuron releases the same neurotransmitter(s) from all of its synapses. This view introduced a strongly reductionist approach to nervous system complexity by assigning each neuron to one of three functional classes (excitatory, inhibitory, or modulatory). Recently, however, several findings have complicated this simple characterization: there is growing evidence that neuronal populations in vertebrate and invertebrate nervous systems use multiple transmitter systems simultaneously. The possibility that neurons may release multiple neurotransmitters was first suggested by Burnstock (1976). Subsequent anatomical studies demonstrated the co-localization of multiple transmitters in single neurons (Hökfelt et al., 1977, 1987, 1998), and functional investigations have shown that many neuronal subtypes can store and release multiple neurotransmitters simultaneously (Granger et al., 2016; Hnasko and Edwards, 2012; Noh et al., 2010; Seal and Edwards, 2006; Vaaga et al., 2014). Nowadays, the concept of neurotransmitter co-release by single neurons is well accepted, and many, if not most, neurons are understood to use multiple transmission. However, the prevalence and physiological roles of co-transmission remain poorly understood, as is the synaptic circuitry involved.

The adult zebrafish spinal cord neurotransmitter atlas presented here is an essential resource for identifying currently unknown subpopulations of spinal neurons and for future comparative studies on spinal circuit organization. Our anatomical mapping revealed a population of adult spinal neurons expressing

both GABA and glycine, as previously demonstrated during zebrafish development (Higashijima et al., 2004a). It is well established that many neurons in the vertebrate spinal cord co-express and release these inhibitory neurotransmitters (Alvarez and Fyffe, 2007; Chery and de Koninck, 1999; Geiman et al., 2002; Taal and Holstege, 1994; Todd et al., 1996; Svensson et al., 2018). Moreover, in keeping with our observations here, it is well established that the vertebrate cholinergic spinal neurons (motoneurons) can co-express and co-release glutamate along with acetylcholine (Bertuzzi et al., 2018; Meister et al., 1993; Mentis et al., 2005; Nishimaru et al., 2005). Interestingly, we also found that spinal cord neurons exhibit extensive co-expression of glutamate and GABA, two neurotransmitters with opposing functions. Although we did not investigate the release of these transmitters in this work, the possible co-release of glutamate and GABA from single nerve terminals in the brain has been demonstrated extensively (Beltrán and Gutiérrez, 2012; Galván and Gutiérrez, 2017; Noh et al., 2010; Root et al., 2014; Shabel et al., 2014; Yoo et al., 2016). Our findings support the existence of multi-transmitter neurons in the zebrafish spinal cord, as was already established in the lamprey spinal cord (Fernández-López et al., 2012) and the mammalian brain (Granger et al., 2017; Tritsch et al., 2016). However, the co-expression and co-release of these diverse transmitter combinations in mammalian spinal neurons has yet to be confirmed. Since the spinal cord is an evolutionarily conserved region of the central nervous system (Arber, 2012; Grillner, 2003; Grillner and Jessell, 2009), our results are probably relevant to organisms of higher phylogenetic order, including mammals. Based on this evolutionary perspective, we suggest that the diversity and complexity of zebrafish spinal neurons is likely to be echoed on larger scales in mammalian spinal systems, enabling better control of far more complex motor behaviors.

Our analysis also shows that the V2a interneurons form a functionally heterogeneous class of neurons that co-express GABA, glycine, or ChAT in addition to glutamate. Although several previous studies on the anatomical and functional organization of the V2a interneurons neglected the possibility that they might co-express and potentially co-release neurotransmitters other than glutamate (Ampatzis et al., 2014; Ausborn et al., 2012; Dougherty and Kiehn, 2010), previous attempts were made for the characterization of their neurotransmitter phenotype (Lundfald et al., 2007). In the developing mammalian spinal cord, most (~80%) of the V2a interneurons were observed to be glutamatergic, and a small fraction (~5%) to be putative glycinergic, but none GABAergic (*GAD$_{67}$:GFP^{+}*; Lundfald et al., 2007). However, these findings cannot exclude the possibility that GABAergic mammalian V2a interneurons exist as they can alternatively use the GAD$_{65}$ as glutamate decarboxylase, which is present in a different set of neurons within the central nervous system (Ma et al., 1994; Feldblum et al., 1995; Lee et al., 2011). Furthermore, in line with our data presented here, a recent single-cell transcriptome analysis of the mammalian spinal cord neurons revealed the presence of the cholinergic vesicular transporter (vAChT), of the vIAAT and the GlyT2 in the V2a interneuron population (Delile et al., 2019). Together this demonstrated diversity of the V2a interneurons can reflect their functional heterogeneity that has been observed before in both zebrafish (Ampatzis et al., 2014; Ausborn et al., 2012; Song et al., 2018) and mice (Al-Mosawie et al., 2007; Zhong et al., 2011). In particular, the V2a interneurons in adult zebrafish form three discrete functional subpopulations that are incrementally recruited at different speeds of locomotion, and their recruitment pattern is not topographically organized (Ampatzis et al., 2014; Ausborn et al., 2012; Song et al., 2018). Although our findings indicate that a small fraction of the V2a interneurons can co-express other classical neurotransmitters in addition to glutamate, it seems very unlikely that these other neurotransmitters are released to control spinal motoneuron activity (Ampatzis et al., 2014; Song et al., 2016, 2018). It seems more likely that these additional neurotransmitters mediate the neuronal interplay needed for the precise operation of the central pattern generators and may also contribute to the establishment of the necessary rostro-caudal delay.

Limitations of the Study

Although the immunodetection and *in situ* hybridization methods have considerable advantages enabling the detailed analysis of the transmitter phenotypes of the spinal neurons, several key limitations remain. First, the immunodetection of the transmitter neural phenotypes is constrained to cell somata. Thus, future functional validation of the co-transmission remains to be determined, in particular, to functionally validate the glutamatergic nature of the spinal cord neurons, as high concentrations of glutamate could exist in metabolically active cells (Storm-Mathisen et al., 1986; Zhang et al., 1991). Second, the fluorescent microscopic analysis is limited to the number of fluorescent probes that are currently available. Thus, our study may be considered conservative and underestimate the full neurotransmitter complexity that exists in the vertebrate spinal neurons. A complete and accurate single-cell transcriptomic analysis will help to overcome this critical limitation. Third, it is essential to be aware that the study here considered the

neurotransmitter phenotypes as fixed. However, neurons can dynamically change their neurotransmitter phenotypes, under both physiological and pathophysiological conditions (Black et al., 1984; Dulcis et al., 2013, 2017; Spitzer, 2015; 2017; Bertuzzi et al., 2018).

METHODS

All methods can be found in the accompanying Transparent Methods supplemental file.

SUPPLEMENTAL INFORMATION

Supplemental Information can be found online at https://doi.org/10.1016/j.isci.2019.09.010.

ACKNOWLEDGMENTS

We thank Drs Shin-Ichi Higashijima, Emre Yaksi, and Harold Burgess for sharing their transgenic animal lines. We also thank Drs. Mario Wullimann, Mark Masino, Konstantinos Meletis, Maria Bertuzzi, and Luca Bartesaghi for their valuable discussion, comments, technical contributions to the project, and assistance in preparing this manuscript. This work was supported by a grant from the Swedish Research Council (2015-03359 to K.A.), StratNeuro (to K.A.), Swedish Brain Foundation (FO2016-0007 and FO2019-0011 to K.A.), STINT (CH2017-7227 to K.A.), Carl Tryggers Foundation (CTS 18:9 to K.A.), Karolinska Institutet and Längmanska kulturfonden (BA17-0390 to K.A.).

AUTHOR CONTRIBUTIONS

K.A. conceived the project and designed the experiments. A.P. and K.A. performed the experiments, analyzed the data, discussed the results, prepared the figures, and wrote the manuscript.

DECLARATION OF INTERESTS

The authors declare no competing interests.

Received: November 22, 2018
Revised: April 24, 2019
Accepted: September 5, 2019
Published: September 27, 2019

REFERENCES

Al-Mosawie, A., Wilson, J.M., and Brownstone, R.M. (2007). Heterogeneity of V2-derived interneurons in the adult mouse spinal cord. Eur. J. Neurosci. *26*, 3003–3015.

Alaynick, W.A., Jessell, T.M., and Pfaff, S.L. (2011). SnapShot: spinal cord development. Cell *146*, 178–178.e1.

Alvarez, F.J., and Fyffe, R.E.W. (2007). The continuing case for the Renshaw cell. J. Physiol. (Lond.) *584*, 31–45.

Alvarez, F.J., Jonas, P.C., Sapir, T., Hartley, R., Berrocal, M.C., Geiman, E.J., Todd, A.J., and Goulding, M. (2005). Postnatal phenotype and localization of spinal cord V1 derived interneurons. J. Comp. Neurol. *493*, 177–192.

Ampatzis, K., Song, J., Ausborn, J., and El Manira, A. (2014). Separate microcircuit modules of distinct v2a interneurons and motoneurons control the speed of locomotion. Neuron *83* (4), 934–943.

Ampatzis, K., Song, J., Ausborn, J., and El Manira, A. (2013). Pattern of innervation and recruitment of different classes of motoneurons in adult zebrafish. J. Neurosci. *33*, 10875–10886.

Antal, M., Berki, A.C., Horvath, L., and O'Donovan, M.J. (1994). Developmental changes in the distribution of gamma-aminobutyric acid-immunoreactive neurons in the embryonic chick lumbosacral spinal cord. J. Comp. Neurol. *343*, 228–236.

Arber, S. (2012). Motor circuits in action: specification, connectivity, and function. Neuron *74*, 975–989.

Ausborn, J., Mahmood, R., and El Manira, A. (2012). Decoding the rules of recruitment of excitatory interneurons in the adult zebrafish locomotor network. Proc. Natl. Acad. Sci. U S A *109*, E3631–E3639.

Barreiro-Iglesias, A., Mysiak, K.S., Adrio, F., Rodicio, M.C., Becker, C.G., Becker, T., and Anadón, R. (2013). Distribution of glycinergic neurons in the brain of glycine transporter-2 transgenic Tg(glyt2:Gfp) adult zebrafish: relationship to brain-spinal descending systems. J. Comp. Neurol. *521*, 389–425.

Beltrán, J.Q., and Gutiérrez, R. (2012). Co-release of glutamate and GABA from single, identified mossy fibre giant boutons. J. Physiol. (Lond.) *590*, 4789–4800.

Bernhardt, R.R., Chitnis, A.B., Lindamer, L., and Kuwada, J.Y. (1990). Identification of spinal neurons in the embryonic and larval zebrafish. J. Comp. Neurol. *302*, 603–616.

Bernhardt, R.R., Patel, C.K., Wilson, S.W., and Kuwada, J.Y. (1992). Axonal trajectories and distribution of GABAergic spinal neurons in wildtype and mutant zebrafish lacking floor plate cells. J. Comp. Neurol. *326*, 263–272.

Bertuzzi, M., Chang, W., and Ampatzis, K. (2018). Adult spinal motoneurons change their neurotransmitter phenotype to control locomotion. Proc. Natl. Acad. Sci. U S A *115*, E9926–E9933.

Björnfors, E.R., and El Manira, A. (2016). Functional diversity of excitatory commissural interneurons in adult zebrafish. Elife *5*, 10875.

Black, I.B., Adler, J.E., Dreyfus, C.F., Jonakait, G.M., Katz, D.M., LaGamma, E.F., and Markey, K.M. (1984). Neurotransmitter plasticity at the molecular level. Science *225*, 1266–1270.

Böhm, U.L., Prendergast, A., Djenoune, L., Nunes Figueiredo, S., Gomez, J., Stokes, C., Kaiser, S., Suster, M., Kawakami, K., Charpentier, M., et al. (2016). CSF-contacting neurons regulate

locomotion by relaying mechanical stimuli to spinal circuits. Nat. Commun. *7*, 10866.

Bradley, S., Tossell, K., Lockley, R., and McDearmid, J.R. (2010). Nitric oxide synthase regulates morphogenesis of zebrafish spinal cord motoneurons. J. Neurosci. *30*, 16818–16831.

Brodin, L., Dale, N., Christenson, J., Storm-Mathisen, J., Hökfelt, T., and Grillner, S. (1990). Three types of GABA-immunoreactive cells in the lamprey spinal cord. Brain Res. *508*, 172–175.

Burnstock, G. (1976). Do some nerve cells release more than one transmitter? Neuroscience *1*, 239–248.

Chaudhry, F.A., Reimer, R.J., Bellocchio, E.E., Danbolt, N.C., Osen, K.K., Edwards, R.H., and Storm-Mathisen, J. (1998). The vesicular GABA transporter, VGAT, localizes to synaptic vesicles in sets of glycinergic as well as GABAergic neurons. J. Neurosci. *18*, 9733–9750.

Chery, N., and de Koninck, Y. (1999). Junctional versus extrajunctional glycine and GABA(A) receptor-mediated IPSCs in identified lamina I neurons of the adult rat spinal cord. J. Neurosci. *19*, 7342–7355.

Crone, S.A., Quinlan, K.A., Zagoraiou, L., Droho, S., Restrepo, C.E., Lundfald, L., Endo, T., Setlak, J., Jessell, T.M., Kiehn, O., and Sharma, K. (2008). Genetic ablation of V2a ipsilateral interneurons disrupts left-right locomotor coordination in mammalian spinal cord. Neuron *60*, 70–83.

Delile, J., Rayon, T., Melchionda, M., Edwards, A., Briscoe, J., and Sagner, A. (2019). Single cell transcriptomics reveals spatial and temporal dynamics of gene expression in the developing mouse spinal cord. Development *146*, https://doi.org/10.1242/dev.173807.

Djenoune, L., Desban, L., Gomez, J., Sternberg, J.R., Prendergast, A., Langui, D., Quan, F.B., Marnas, H., Auer, T.O., Rio, J.-P., et al. (2017). The dual developmental origin of spinal cerebrospinal fluid-contacting neurons gives rise to distinct functional subtypes. Sci. Rep. *7*, 719.

Dougherty, K.J., and Kiehn, O. (2010). Firing and cellular properties of V2a interneurons in the rodent spinal cord. J. Neurosci. *30*, 24–37.

Dulcis, D., Jamshidi, P., Leutgeb, S., and Spitzer, N.C. (2013). Neurotransmitter switching in the adult brain regulates behavior. Science *340*, 449–453.

Dulcis, D., Lippi, G., Stark, C.J., Do, L.H., Berg, D.K., and Spitzer, N.C. (2017). Neurotransmitter switching regulated by miRNAs controls changes in social preference. Neuron *95*, 1319–1333.e5.

Eccles, J.C., Fatt, P., and Koketsu, K. (1954). Cholinergic and inhibitory synapses in a pathway from motor-axon collaterals to motoneurons. J. Physiol. *126*, 524–562.

Eklöf-Ljunggren, E., Haupt, S., Ausborn, J., Dehnisch, I., Uhlén, P., Higashijima, S.-I., and El Manira, A. (2012). Origin of excitation underlying locomotion in the spinal circuit of zebrafish. Proc. Natl. Acad. Sci. U S A *109*, 5511–5516.

Feldblum, S., Dumoulin, A., Anoal, M., Sandillon, F., and Privat, A. (1995). Comparative distribution of GAD65 and GAD67 mRNAS and proteins in the rat spinal cord supports a differential regulation of these two glutamate decarboxylases in vivo. J. Neurosci. Res. *42*, 742–757.

Fernández-López, B., Villar-Cerviño, V., Valle-Maroto, S.M., Barreiro-Iglesias, A., Anadón, R., and Rodicio, M.C. (2012). The glutamatergic neurons in the spinal cord of the sea lamprey: an in situ hybridization and immunohistochemical study. PLoS One *7*, e47898.

Galván, E.J., and Gutiérrez, R. (2017). Target-dependent compartmentalization of the corelease of glutamate and GABA from the mossy fibers. J. Neurosci. *37*, 701–714.

Geiman, E.J., Zheng, W., Fritschy, J.-M., and Alvarez, F.J. (2002). Glycine and GABA(A) receptor subunits on Renshaw cells: relationship with presynaptic neurotransmitters and postsynaptic gephyrin clusters. J. Comp. Neurol. *444*, 275–289.

Goulding, M. (2009). Circuits controlling vertebrate locomotion: moving in a new direction. Nat. Rev. Neurosci. *10*, 507–518.

Granger, A.J., Mulder, N., Saunders, A., and Sabatini, B.L. (2016). Cotransmission of acetylcholine and GABA. Neuropharmacology *100*, 40–46.

Granger, A.J., Wallace, M.L., and Sabatini, B.L. (2017). Multi-transmitter neurons in the mammalian central nervous system. Curr. Opin. Neurobiol. *45*, 85–91.

Grillner, S., and Jessell, T.M. (2009). Measured motion: searching for simplicity in spinal locomotor networks. Curr. Opin. Neurobiol. *19*, 572–586.

Grillner, S.S. (2003). The motor infrastructure: from ion channels to neuronal networks. Nat. Rev. Neurosci. *4*, 573–586.

Hale, M.E., Ritter, D.A., and Fetcho, J.R. (2001). A confocal study of spinal interneurons in living larval zebrafish. J. Comp. Neurol. *437*, 1–16.

Hayashi, M., Hinckley, C.A., Driscoll, S.P., Moore, N.J., Levine, A.J., Hilde, K.L., Sharma, K., and Pfaff, S.L. (2018). Graded arrays of spinal and supraspinal V2a interneuron subtypes underlie forelimb and hindlimb motor control. Neuron *97*, 869–884.

Higashijima, S.-I., Mandel, G., and Fetcho, J.R. (2004a). Distribution of prospective glutamatergic, glycinergic, and GABAergic neurons in embryonic and larval zebrafish. J. Comp. Neurol. *480*, 1–18.

Higashijima, S.-I., Schaefer, M., and Fetcho, J.R. (2004b). Neurotransmitter properties of spinal interneurons in embryonic and larval zebrafish. J. Comp. Neurol. *480*, 19–37.

Hnasko, T.S., and Edwards, R.H. (2012). Neurotransmitter corelease: mechanism and physiological role. Annu. Rev. Physiol. *74*, 225–243.

Hökfelt, T., Elfvin, L.G., Elde, R., Schultzberg, M., Goldstein, M., and Luft, R. (1977). Occurrence of somatostatin-like immunoreactivity in some peripheral sympathetic noradrenergic neurons. Proc. Natl. Acad. Sci. U S A *74*, 3587–3591.

Hökfelt, T., Fuxe, K., and Pernow, N. (1987). Coexistence of peptides with classical neurotransmitters. Experientia *43*, 768–780.

Hökfelt, T., Xu, Z.Q., Shi, T.J., Holmberg, K., and Zhang, X. (1998). Galanin in ascending systems: focus on coexistence with 5-hydroxytryptamine and noradrenaline. Ann. N. Y. Acad. Sci. *863*, 252–263.

Jessell, T.M. (2000). Neuronal specification in the spinal cord: inductive signals and transcriptional codes. Nat. Rev. Genet. *1*, 20–29.

Joshi, K., Lee, S., Lee, B., Lee, J.W., and Lee, S.K. (2009). LMO4 controls the balance between excitatory and inhibitory spinal V2 interneurons. Neuron *61*, 839–851.

Kiehn, O. (2011). Development and functional organization of spinal locomotor circuits. Curr. Opin. Neurobiol. *21*, 100–109.

Kiehn, O. (2016). Decoding the organization of spinal circuits that control locomotion. Nat. Rev. Neurosci. *17*, 224–238.

Kimura, Y., Okamura, Y., and Higashijima, S.-I. (2006). alx, a zebrafish homolog of Chx10, marks ipsilateral descending excitatory interneurons that participate in the regulation of spinal locomotor circuits. J. Neurosci. *26*, 5684–5697.

Kimura, Y., Satou, C., and Higashijima, S.-I. (2008). V2a and V2b neurons are generated by the final divisions of pair-producing progenitors in the zebrafish spinal cord. Development *135*, 3001–3005.

Lee, H.J., Choi, J.H., Ahn, J.H., Lee, C.H., Yoo, K.-Y., Hwang, I.K., Kim, J.S., Kim, C., Lee, Y.L., Shin, H.-C., et al. (2011). Comparison of GAD65 and 67 immunoreactivity in the lumbar spinal cord between young adult and aged dogs. Neurochem. Res. *36*, 435–442.

Liao, J.C., and Fetcho, J.R. (2008). Shared versus specialized glycinergic spinal interneurons in axial motor circuits of larval zebrafish. J. Neurosci. *28*, 12982–12992.

Lundfald, L., Restrepo, C.E., Butt, S.J., Peng, C.Y., Droho, S., Endo, T., Zeilhofer, H.U., Sharma, K., and Kiehn, O. (2007). Phenotype of V2-derived interneurons and their relationship to the axon guidance molecule EphA4 in the developing mouse spinal cord. Eur. J. Neurosci. *26*, 2989–3002.

Ma, W., Behar, T., Chang, L., and Barker, J.L. (1994). Transient increase in expression of GAD65 and GAD67 mRNA during postnatal development of rat spinal cord. J. Comp. Neurol. *346*, 151–160.

Mahmood, R., Restrepo, C.E., and El Manira, A. (2009). Transmitter phenotypes of commissural interneurons in the lamprey spinal cord. Neuroscience *164*, 1057–1067.

McLean, D.L., and Fetcho, J.R. (2004). Ontogeny and innervation patterns of dopaminergic, noradrenergic, and serotonergic neurons in larval zebrafish. J. Comp. Neurol. *480*, 38–56.

McLean, D.L., and Fetcho, J.R. (2009). Spinal interneurons differentiate sequentially from those driving the fastest swimming movements in larval

zebrafish to those driving the slowest ones. J. Neurosci. *29*, 13566–13577.

McLean, D.L., Fan, J., Higashijima, S.-I., and Fetcho, J.R. (2007). A topographic map of recruitment in spinal cord. Nature *446*, 71–75.

McLean, D.L., Masino, M.A., Koh, I.Y., Lindquist, W.B., and Fetcho, J.R. (2008). Continuous shifts in the active set of spinal interneurons during changes in locomotor speed. Nat. Neurosci. *11*, 1419–1429.

Meister, B., Arvidsson, U., Zhang, X., Jacobsson, G., Villar, M.J., and Hökfelt, T. (1993). Glutamate transporter mRNA and glutamate-like immunoreactivity in spinal motoneurones. Neuroreport *5*, 337–340.

Menelaou, E., VanDunk, C., and McLean, D.L. (2014). Differences in the morphology of spinal V2a neurons reflect their recruitment order during swimming in larval zebrafish. J. Comp. Neurol. *522*, 1232–1248.

Mentis, G.Z., Alvarez, F.J., Bonnot, A., Richards, D.S., González-Forero, D., Zerda, R., and O'Donovan, M.J. (2005). Noncholinergic excitatory actions of motoneurons in the neonatal mammalian spinal cord. Proc. Natl. Acad. Sci. U S A *102*, 7344–7349.

Nishimaru, H., Restrepo, C.E., Ryge, J., Yanagawa, Y., and Kiehn, O. (2005). Mammalian motor neurons corelease glutamate and acetylcholine at central synapses. Proc. Natl. Acad. Sci. U S A *102*, 5245–5249.

Noh, J., Seal, R.P., Garver, J.A., Edwards, R.H., and Kandler, K. (2010). Glutamate co-release at GABA/glycinergic synapses is crucial for the refinement of an inhibitory map. Nat. Neurosci. *13*, 232–238.

Phelps, P.E., Barber, R.P., Brennan, L.A., Maines, V.M., Salvaterra, P.M., and Vaughn, J.E. (1990). Embryonic development of four different subsets of cholinergic neurons in rat cervical spinal cord. J. Comp. Neurol. *291*, 9–26.

Pombal, M.A., Marín, O., and González, A. (2001). Distribution of choline acetyltransferase-immunoreactive structures in the lamprey brain. J. Comp. Neurol. *431*, 105–126.

Restrepo, C.E., Lundfald, L., Szabó, G., Erdélyi, F., Zeilhofer, H.U., Glover, J.C., and Kiehn, O. (2009). Transmitter-phenotypes of commissural interneurons in the lumbar spinal cord of newborn mice. J. Comp. Neurol. *517*, 177–192.

Rogawski, M.A., and Barker, J.L. (1986). Neurotransmitter Actions in the Vertebrate Nervous System (Springer), p. 511.

Root, D.H., Mejias-Aponte, C.A., Zhang, S., Wang, H.-L., Hoffman, A.F., Lupica, C.R., and Morales, M. (2014). Single rodent mesohabenular axons release glutamate and GABA. Nat. Neurosci. *17*, 1543–1551.

Satou, C., Kimura, Y., and Higashijima, S.-I. (2012). Generation of multiple classes of V0 neurons in zebrafish spinal cord: progenitor heterogeneity and temporal control of neuronal diversity. J. Neurosci. *32*, 1771–1783.

Schwartz, J.H. (2000). Neurotransmitters. In Principles of Neural Science, E.R. Kandel, J.H. Schwartz, and T.M. Jessell, eds. (Elsevier), pp. 280–295.

Seal, R.P., and Edwards, R.H. (2006). Functional implications of neurotrans- mitter co-release: glutamate and GABA share the load. Curr. Opin. Pharmacol. *6*, 114–119.

Shabel, S.J., Proulx, C.D., Piriz, J., and Malinow, R. (2014). Mood regulation. GABA/glutamate co-release controls habenula output and is modified by antidepressant treatment. Science *345*, 1494–1498.

Shigeri, Y., Seal, R.P., and Shimamoto, K. (2004). Molecular pharmacology of glutamate transporters, EAATs and VGLUTs. Brain Res. Brain Res. Rev. *45*, 250–265.

Song, J., Ampatzis, K., Björnfors, E.R., and El Manira, A. (2016). Motor neurons control locomotor circuit function retrogradely via gap junctions. Nature *529*, 399–402.

Song, J., Dahlberg, E., and El Manira, A. (2018). V2a interneuron diversity tailors spinal circuit organization to control the vigor of locomotor movements. Nat. Commun. *9*, 3370.

Spitzer, N.C. (2015). Neurotransmitter switching? no surprise. Neuron *86*, 1131–1144.

Spitzer, N.C. (2017). Neurotransmitter switching in the developing and adult brain. Annu. Rev. Neurosci. *40*, 1–19.

Stil, A., and Drapeau, P. (2016). Neuronal labeling patterns in the spinal cord of adult transgenic Zebrafish. Dev. Neurobiol. *76*, 642–660.

Storm-Mathisen, J., Ottersen, O.P., Fu-Long, T., Gundersen, V., Laake, J.H., and Nordbø, G. (1986). Metabolism and transport of amino acids studied by immunocytochemistry. Med. Biol. *64*, 127–132.

Sueiro, C., Carrera, I., Molist, P., Rodríguez-Moldes, I., and Anadón, R. (2004). Distribution and development of glutamic acid decarboxylase immunoreactivity in the spinal cord of the dogfish *Scyliorhinus canicula* (elasmobranchs). J. Comp. Neurol. *478*, 189–206.

Svensson, E., Williams, M.J., and Schiöth, H.B. (2018). Neural cotransmission in spinal circuits governing locomotion. Trends Neurosci. *41*, 540–550.

Taal, W., and Holstege, J.C. (1994). GABA and glycine frequently colocalize in terminals on cat spinal motoneurons. Neuroreport *5*, 2225–2228.

Todd, A.J., Watt, C., Spike, R.C., and Sieghart, W. (1996). Colocalization of GABA, glycine, and their receptors at synapses in the rat spinal cord. J. Neurosci. *16*, 974–982.

Tritsch, N.X., Granger, A.J., and Sabatini, B.L. (2016). Mechanisms and functions of GABA co-release. Nat. Rev. Neurosci. *17*, 139–145.

Unwin, N. (1993). Neurotransmitter action: opening of ligand-gated ion channels. Cell *72*, 31–41.

Vaaga, C.E., Borisovska, M., and Westbrook, G.L. (2014). Dual-transmitter neurons: functional implications of co-release and co-transmission. Curr. Opin. Neurobiol. *29*, 25–32.

Wéber, I., Veress, G., Szucs, P., Antal, M., and Birinyi, A. (2007). Neurotransmitter systems of commissural interneurons in the lumbar spinal cord of neonatal rats. Brain Res. *1178*, 65–72.

Weihe, E., Tao-Cheng, J.H., Schäfer, M.K., Erickson, J.D., and Eiden, L.E. (1996). Visualization of the vesicular acetylcholine transporter in cholinergic nerve terminals and its targeting to a specific population of small synaptic vesicles. Proc. Natl. Acad. Sci. USA *93*, 3547–3552.

Wojcik, S.M., Katsurabayashi, S., Guillemin, I., Friauf, E., Rosenmund, C., Brose, N., and Rhee, J.S. (2006). A shared vesicular carrier allows synaptic corelease of GABA and glycine. Neuron *50*, 575–587.

Yoo, J.H., Zell, V., Gutierrez-Reed, N., Wu, J., Ressler, R., Shenasa, M.A., Johnson, A.B., Fife, K.H., Faget, L., and Hnasko, T.S. (2016). Ventral tegmental area glutamate neurons co-release GABA and promote positive reinforcement. Nat. Commun. *7*, 13697.

Zhang, N.H., Laake, J., Nagelhus, E., Storm-Mathisen, J., and Ottersen, O.P. (1991). Distribution of glutamine-like immunoreactivity in the cerebellum of rat and baboon (*Papio anubis*) with reference to the issue of metabolic compartmentation. Anat. Embryol. *184*, 213–223.

Zhong, G., Sharma, K., and Harris-Warrick, R.M. (2011). Frequency-dependent recruitment of V2a interneurons during fictive locomotion in the mouse spinal cord. Nat. Commun. *2*, 274–310.

ISCI, Volume *19*

Supplemental Information

Large-Scale Analysis of the Diversity and Complexity of the Adult Spinal Cord Neurotransmitter Typology

Andrea Pedroni and Konstantinos Ampatzis

Supplemental Information

Large scale analysis of the diversity and complexity of the adult spinal cord neurotransmitter typology

Andrea Pedroni and Konstantinos Ampatzis

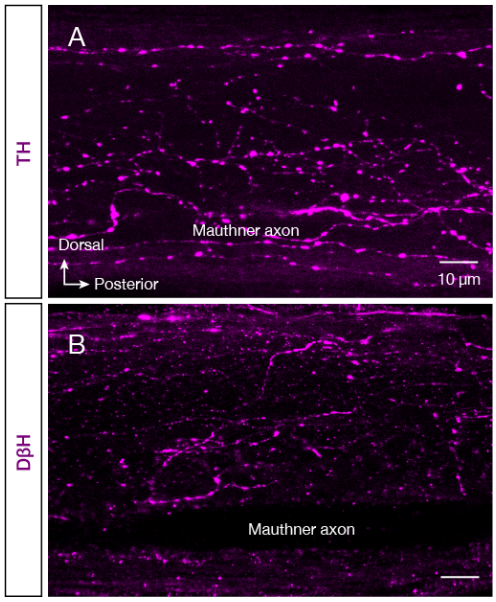

Figure S1. Lack of spinal dopaminergic and noradrenergic neurons, Related to Figure 2.
(A-B) Representative whole mount confocal images showing that only dopaminergic (TH^+) and noradrenergic ($D\beta H^+$) neuronal processes are detectable in the adult zebrafish spinal cord.

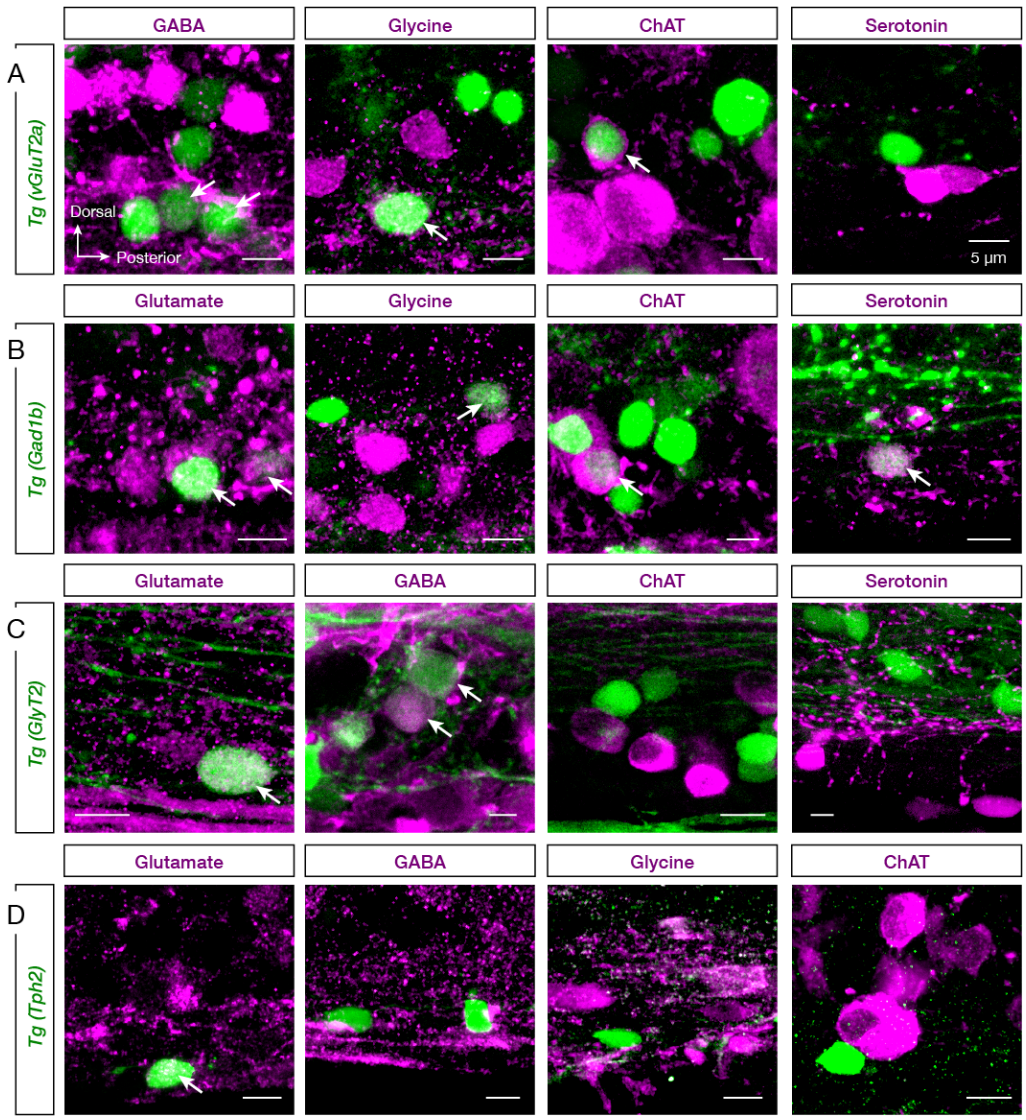

Figure S2. The presence of co-expressing neurons in transgenic animal lines, Related to Figure 4. (A-D) Representative whole mount images from transgenic (*GlyT2*, *vGluT2a*, *Gad1b*, *Tph2*; green) adult zebrafish spinal cord preparations, immunolabeled for glutamate, GABA, glycine, ChAT and serotonin (magenta). Arrows indicate the double labeled cells.

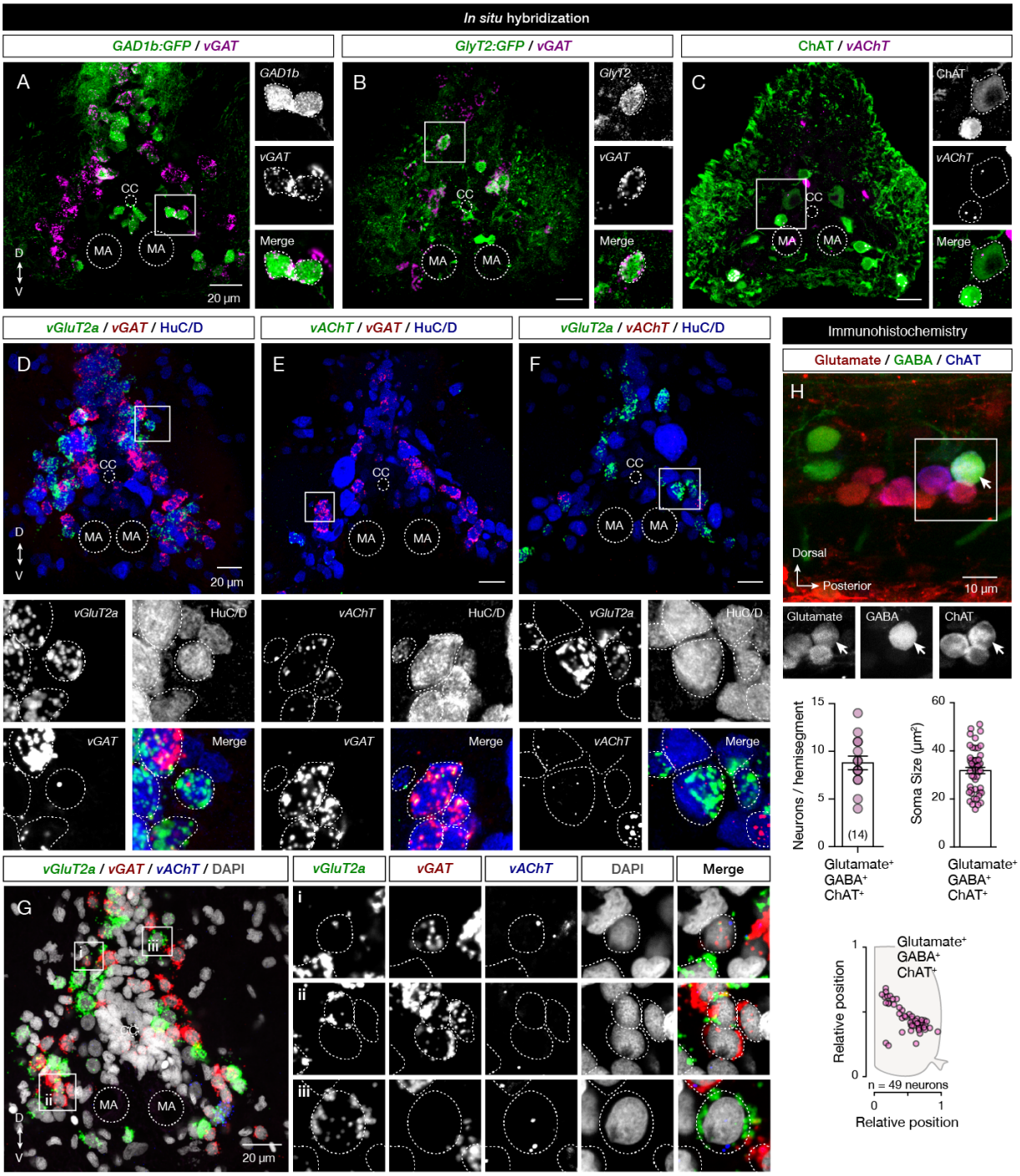

Figure S3. *In situ* detection of the neurotransmitter's vesicular transporters, Related to Figure 4.
(A-B) Confocal photomicrographs of transversal sections of the adult zebrafish spinal cord showing the presence of the *vGAT* mRNA in all the putative GABAergic (*GAD1b*) and Glycinergic (*GlyT2*) neurons.
(C) *In situ* hybridization reveals a small number of the vesicular acetylcholine transporter (*vAChT*) mRNA in all the cholinergic spinal neurons (ChAT$^+$).
(D-F) Co-localization of different vesicular transporter mRNAs in adult zebrafish spinal cord.
(G) Representative *in situ* hybridization for all the vesicular transporters (*vGluT2a*, *vGAT* and *vAChT*) mRNA showing a co-localization in the adult zebrafish spinal cord neurons.
(H) Triple immunolabeling confirms the existence of multi-expressing, glutamate (red), GABA (green) and ChAT (blue) neurons. Arrow indicates the triple labeled neuron. Quantification of the number and spatial distribution of cholinergic neurons co-expressing simultaneously glutamate and GABA in the adult zebrafish spinal cord hemisegment (segment 15). Quantification of the ChAT$^+$Glutamate$^+$GABA$^+$ neurons soma size.
Dotted lines represent the borders of the neurons. Data are presented as mean ± SEM. CC, central canal; MA, Mauthner axon.

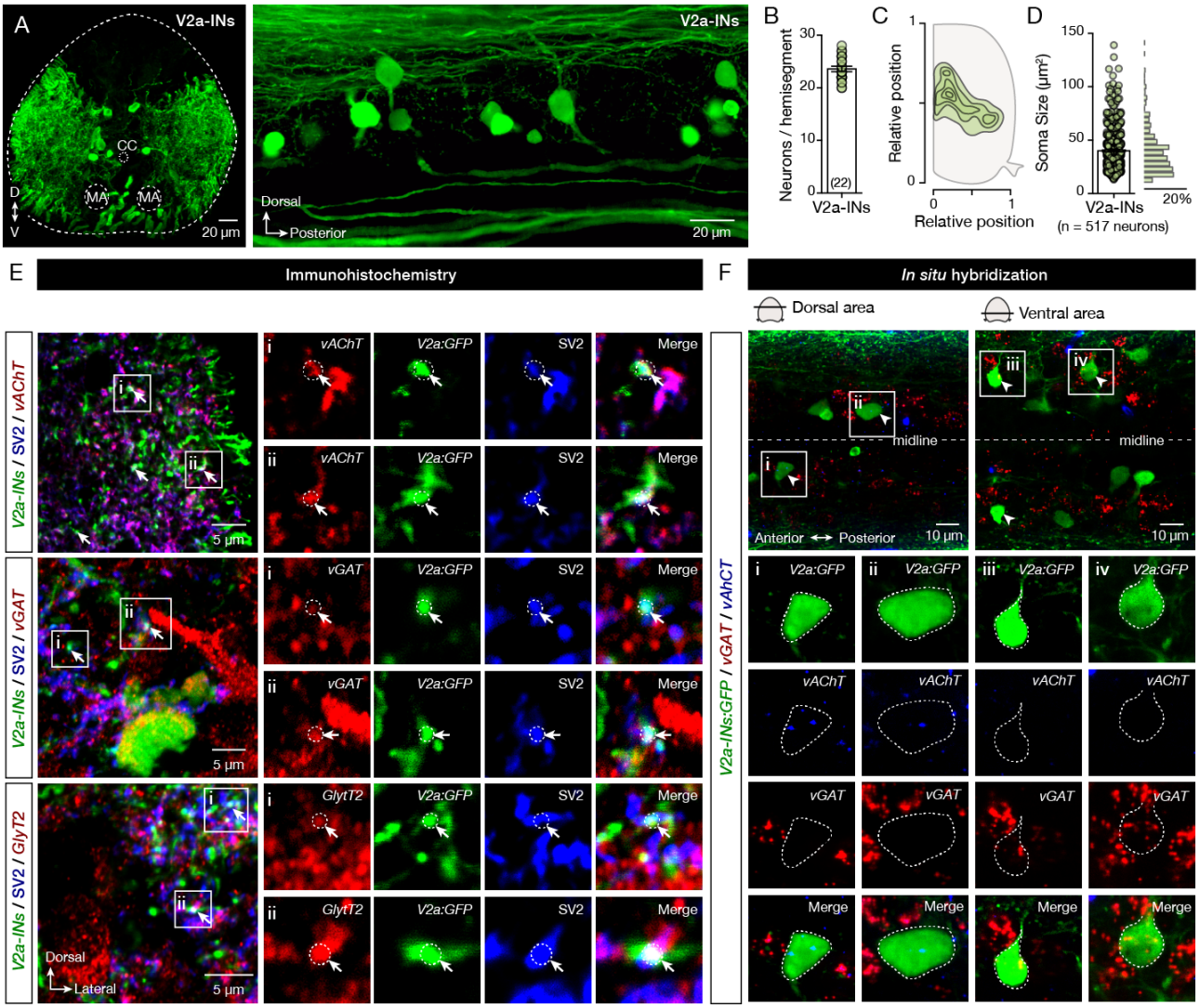

Figure S4. V2a interneuron analysis, Related to Figure 5.

(A) Transverse section and whole mount adult zebrafish spinal cord showing the distribution of the V2a interneuron population.

(B) Quantification of the number of V2a interneurons in adult spinal cord hemisegment (segment 15).

(C) Spatial distribution of the V2a interneurons with the medio-lateral and dorso-ventral density plot.

(D) Quantification and distribution analysis of the V2a interneuron soma sizes (*n* = 517 neurons).

(E) Confocal photomicrographs of transversal sections of the adult zebrafish spinal cord showing the colocalization of the presynaptic V2a interneuron terminals (GFP$^+$/SV2$^+$) with the vesicular acetylcholine transporter (vAChT), the vesicular GABA and glycine transporter (vGAT) or with the glycinergic transporter (GlyT2). Arrows indicate the triple co-localization.

(F) Whole mount *in situ* hybridization reveals the co-existence of the different vesicular neurotransmitter transporter mRNAs (*vAChT* or *vGAT*) in the V2a (GFP$^+$) interneurons in the expected relative locations (dorsal, ventral) within the adult zebrafish spinal cord. Arrowheads indicate the double labeled neurons.

Data are presented as mean ± SEM. CC, central canal; MA, Mauthner axon.

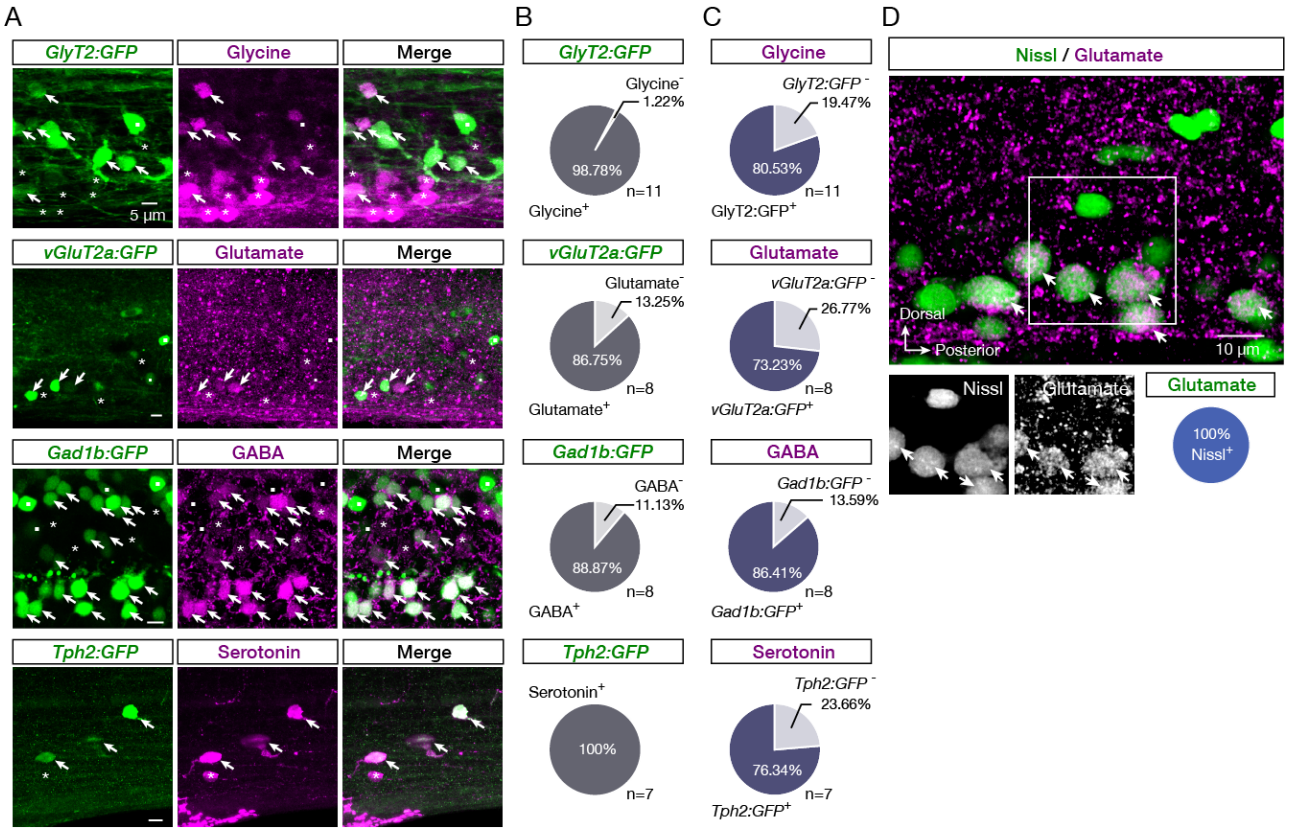

Figure S5. Transgenic lines capture part of the labeled neuronal populations, Related to Figure 2.
(A) Representative immunofluorescent whole-mount images showing immunostained neurons in the spinal cord of transgenic zebrafish with glycinergic (*GlyT2*), glutamatergic (*vGluT2a*), GABAergic (*Gad1b*) or serotonergic (*Tph2*) neurons genetically labelled (green). Asterisks denote the immunopositive neurons that do not express GFP, dots indicate the GFP expressing neurons that are not immunoreactive and arrows identify double labelled neurons.
(B) Quantification of the percentage of immunolabeled neurons that express GFP.
(C) Quantification of the percentage of GFP^+ neurons that are labeled with antibodies.
(D) Representative whole mount image of adult zebrafish spinal cord, immunolabeled for glutamate (magenta) with neurons identified by Nissl staining (green). Arrows indicate the double labeled cells.

TABLE S1. Antibodies Used[1], Related to Figures 1-5.

Antigen	Host	Source	Code	Dilution
Primary				
ChAT	Goat	Millipore	AB144P; RRID: AB_2079751	1:150
DβH	Rabbit	Millipore	AB1538; RRID: AB_90751	1:250
Elav3+4 (HuC/D)	Rabbit	GeneTex	GTX128365; RRID: AB_	1:500
GABA	Rabbit	Sigma	A2052; RRID: AB_477652	1:2000
GABA	Mouse	From Prof. P. Streit; RRID: AB_2314450		1:700
Glutamate	Rabbit	Sigma	G6642; RRID: AB_259946	1:6000
Glycine	Rat	ImmunoSolutions	IG1002; RRID: AB_10013222	1:1000
Serotonin	Rabbit	Sigma	S5545; RRID: AB_477522	1:4000
Serotonin	Guinea Pig	From Prof. A. Verhofstadt		1:2500
TH	Mouse	Millipore	MAB318; RRID: AB_2201528	1:800
GFP	Chicken	Abcam	AB13970; RRID: AB_300798	1:500
vGAT	Rabbit	Synaptic Systems	131 002; RRID: AB_887871	1:300
GlyT2	Rabbit	Alomone labs	AGT-012; RRID: AB_11121049	1:200
vAChT	Guinea Pig	Millipore	AB1588; RRID: AB_11214110	1:1000
SV2	Mouse	DSHB	SV2; RRID: AB_2315387	1:200
Secondary				
Chicken IgY-488	Goat	ThermoFisher	A-11039; RRID: AB_2534096	1:500
Chicken IgY-FITC	Rabbit	ThermoFisher	SA1-9511; RRID: AB_1075130	1:500
Goat IgG-568	Donkey	ThermoFisher	A-11057; RRID: AB_2534104	1:500
Goat IgG-488	Donkey	ThermoFisher	A-11055; RRID: AB_2534102	1:500
Goat IgG-647	Donkey	ThermoFisher	A-21447; RRID: AB_2535864	1:500
Guinea Pig IgG-568	Goat	ThermoFisher	A-11075; RRID: AB_2534119	1:500
Mouse IgG-647	Donkey	ThermoFisher	A-31571; RRID: AB_162542	1:500
Mouse IgG-568	Goat	ThermoFisher	A-11004; RRID: AB_2534072	1:500
Mouse IgG-488	Donkey	ThermoFisher	A-21202; RRID: AB_141607	1:500
Rabbit IgG-488	Donkey	ThermoFisher	A-21206; RRID: AB_2535792	1:500
Rabbit IgG-647	Donkey	ThermoFisher	A-31573; RRID: AB_2536183	1:500
Rabbit IgG-568	Donkey	ThermoFisher	A-10042; RRID: AB_2534017	1:500
Rat IgG-550	Donkey	ThermoFisher	SA5-10027; RRID: AB_2556607	1:500
Rat IgG-568	Goat	ThermoFisher	A-11077; RRID: AB_2534121	1:500

[1]ChAT, choline-acetyltransferase; DβH, dopamine beta-hydroxylase; GABA, γ-aminobutyric acid; GFP, green fluorescent protein; GlyT2, glycine transporter 2; TH, tyrosine hydroxylase; SV2, synaptic vesicle glycoprotein 2A; vAChT, vesicular acetylcholine transporter; vGAT, vesicular GABA transporter.

Transparent methods

Experimental animals

All animals were raised and kept in a core facility at the Karolinska Institute according to established procedures. Adult zebrafish (*Danio rerio*; *n* = 635; 9-10 weeks old; length: 16-19 mm; weight: 0.03-0.05 g) wild type (AB/Tübingen), and *Tg*(*vGluT2a:GFP; vGluT2a:DsRed; Gad1b:GFP; Gad1b:DsRed; GlyT2:GFP; Tph2:Gal4^{y228}/UAS:GFP; Chx10:GFP^{nns1}*) lines of either sex (males and females) where used in this study. All experimental protocols were approved by the local Animal Research Ethical Committee, Stockholm (Ethical permit no. 9248-2017) and were performed in accordance with EU guidelines for the care and use of laboratory animals (86/609/CEE). All efforts were made to utilize only the minimum number of experimental animals necessary to produce reliable scientific data.

Immunohistochemistry

All animals were deeply anesthetized with tricaine methane sulfonate (MS-222, Sigma-Aldrich, E10521). The spinal cords were then extracted and fixed in 4% paraformaldehyde (PFA) and 5% saturated picric acid (Sigma-Aldrich, P6744) in phosphate buffer saline (PBS) (0.01M; pH = 7.4, Santa Cruz Biotech., CAS30525-89-4) at 4°C for 2-14h. We performed immunolabeling in both whole mount spinal cords and in cryosections. For cryosections, the tissue was removed carefully and cryoprotected overnight in 30% (w/v) sucrose in PBS at 4°C, embedded in OCT Cryomount (Histolab, 45830), rapidly frozen in dry-ice-cooled isopentane (2-methylbutane; Sigma-Aldrich, 277258) at approximately –35°C, and stored at –80°C until use. Transverse coronal plane cryosections (thickness: 25 µm) of the tissue were collected and processed for immunohistochemistry. In all cases (whole mount and cryosections) the tissue was washed three times for 5 min in PBS (0.01M; pH = 7.4, Santa Cruz Biotech., SC24946). Nonspecific protein binding sites were blocked with 4% normal donkey serum (NDS; Sigma-Aldrich, D9663) with 1% bovine serum albumin (BSA; Sigma-Aldrich, A2153) and 1% Triton X-100 (Sigma-Aldrich, T8787) in PBS for 1 h at room temperature (RT). Primary antibodies (Table S1) were diluted in 1% of blocking solution and applied for 1-3 days at 4°C. After thorough buffer rinses the tissues were then incubated with the appropriate secondary antibodies (Table S1) diluted 1:500 or with streptavidin conjugated to Alexa Fluor 488 (1:500, ThermoFisher, S32354) Alexa Fluor 555 (1:500, ThermoFisher, S32355) or Alexa Fluor 647 (1:500, ThermoFisher, S32357) in 1% Triton X-100 (Sigma-Aldrich, T8787) in PBS overnight at 4°C. Afterwards, the tissue was thoroughly rinsed in PBS and cover-slipped with fluorescent hard medium (VectorLabs; H-1400) on gelatine-coated microscope slides.

For the anti-GABA antisera raised in mouse (Table S1), the tissue was fixed in 4% paraformaldehyde (PFA) containing 0.2% glutaraldehyde (Sigma-Aldrich, G5882) and 5% saturated picric acid in phosphate buffer saline (PBS; 0.01M; pH = 7.4) at 4°C for 10h. Finally, dual and triple neurotransmitter antibody stainings were performed in a sequential manner.

Antibody specificity

The antisera in this study have been widely and successfully used previously in zebrafish to identify and describe the transmitter phenotype of neurons (anti-ChAT: Berg et al., 2018; Bertuzzi and Ampatzis 2018; Bertuzzi et al., 2018; Clemente et al., 2004; Mueller et al., 2004; Moly et al., 2014; Ohnmacht et al., 2016; Reimer et al., 2008; anti-GABA: Berg et al., 2018; Djenoune et al., 2017; Higashijima et al., 2004; Moly et al., 2014; Montgomery et al., 2016; Mueller et al., 2006; anti-Glycine: Berg et al., 2018; Moly et al., 2014; anti-Serotonin: Berg et al., 2018; Kuscha et al., 2012; McPherson et al., 2016; Montgomery et al., 2016; anti-TH: Ampatzis et al., 2008; Ampatzis and Dermon 2010; Rink and Wullimann, 2004; anti-DβH: Ampatzis et al., 2008), and the green fluorescent protein (anti-GFP: Barreiro-Iglesias et al., 2013; Böhm et al., 2016; Kuscha et al., 2012).

To evaluate the antibody specificity, adjacent sections or additional whole mount spinal cords were used in the absence of either primary or secondary antibody. In all cases no residual immunolabeling was detected. In addition, pre-incubation of the neurotransmitter antibodies used in this study with their corresponding antigen (100 µM - 400 µM; GABA (Sigma-Aldrich, A2129), glutamate (Sigma-Aldrich, G3291), glycine (Sigma-Aldrich, G6761), and serotonin (Sigma-Aldrich, 14927) for 1h at RT, eliminated any immunoreactivity.

To further confirm that our antibody immunodetections faithfully represented the neurotransmitter expression of spinal cord neurons, we performed a series of control experiments using transgenic animal lines (*vGluT2a, Gad1b, GlyT2, and Tph2*) combined with immunolabeling. We found that the vast majority or all of the neurons expressing the green fluorescent protein (GFP or DsRed) in either the vesicular

glutamate transporter *vGluT2a*, a marker for glutamatergic excitatory neurons, the GABAergic inhibitory neuron marker *Gad1b*, the glycinergic neuronal marker *GlyT2* or the *Tph2* promoter for serotonergic neurons were immunolabeled with the anti-glutamate, anti-GABA, anti-glycine and anti-serotonin antibodies, respectively (Figure S5A-S5B). We also observed that immunostaining revealed more neurons than those expressing GFP (Glutamate^{+}*vGluT2a*$^{-}$: 26.77 ± 1.527%, *n* = 8; GABA^{+}*Gad1b*$^{-}$: 13.59 ± 1.134%, *n* = 8; Glycine^{+}*GlyT2*$^{-}$: 19.47 ± 0.449%, *n* = 11; Serotonin^{+}*Tph2*$^{-}$: 23.66 ± 1.723%, *n* = 7; Figure S5C). These findings suggest a differential expression of the glutamatergic vesicular transporter vGluT2a from the vGluT1 (in zebrafish spinal motoneurons, Bertuzzi et al., 2018) and/or vGlut3 glutamatergic neurons. Similarly, these findings propose the existence of GABAergic neurons that use the alternative GAD1a and/or GAD2 as a glutamate decarboxycase enzyme and finally the presence of GlyT1 glycinergic neurons. This observed discrepancy between the immunolabelling and the reporter zebrafish lines signify that although the transgenic zebrafish lines consistently label the neurons of the expected neurotransmitter phenotype, they do not mark all neurons within a population. In addition, we used the transgenic animal lines as described above combined with single immunostaining for glutamate, GABA, glycine, ChAT, and serotonin. We observed, that similar to dual immunodetections, the vast majority of the different combinations of co-expression in spinal cord neurons (Figure S2). Regarding the specificity and reliability of the anti-glutamate immunodetection, we performed additional experiments to evaluate whether the glutamate^{+} cells are actually excitatory neurons, as glial cells can also store and release glutamate (Angulo et al., 2004; Hamilton and Attwell, 2010). Double staining with the anti-glutamate antisera and the NeuroTrace 500/525 Green fluorescent Nissl stain (ThermoFisher, N21480) showed that all the immunolabeled are indeed neurons (Figure S5D).

RNAscope *in situ* hybridization

RNAscope *In situ* hybridization experiments shown in Figures S3 and S4, were performed according to manufacturer's instructions in cryosections and in whole mound spinal cord preparations. The vesicular neurotransmitter transporter mRNAs were detected using RNAscope (Advanced Cell Diagnostics) zebrafish designed target probes (*slc17a6b,* also known as *vGluT2a,* Cat# 300031; *slc18a3b*, also known as *vAChT*, Cat# 300031-C2; *slc32a1,* also known as *vGAT* or *vIAAT*, Cat# 300031-C3). Following the *in situ* hybridization, cell nuclei and cell body were revealed using respectively the DAPI staining and anti-Elav 3+4 (HuC/D) immunodetection. In V2a interneuron (*Chx10:GFP*^{nns1}), glutamate decarboxylase 1b transgenic (*GAD1b:GFP*), and in glycine transporter 2 (*GlyT2:GFP*) transgenic zebrafish line, the tissue was further processed for immunohistochemical detection of the GFP in the same way as in all immunodetections (see above, "Immunohistochemistry" section). The tissue was processed and mounted on Thermo Scientific™Superfrost Plus™Adhesion microscope slides and cover-slipped with anti-fade fluorescent mounting medium (Vectashield Hard Set, VectorLabs; H-1400).

Ascending and descending neuron labeling

Zebrafish (*n* = 70) of either sex were anesthetized in 0.03% tricaine methane sulfonate (MS-222, Sigma-Aldrich, E10521). Retrograde labeling of ascending and descending spinal cord neurons located in the spinal segment 15 was performed using dye injections with biotinylated dextran (3000 MW; ThermoFisher, D7135) into segments 10 or 20 respectively. Afterwards, all animals were kept alive for at least 24h to allow retrograde transport of the tracer. Afterwards, all animals were deeply anesthetized with 0.1% MS-222. The spinal cords were dissected and fixed in 4% paraformaldehyde (PFA) and 5% saturated picric acid (Sigma-Aldrich, P6744) in phosphate buffer saline (PBS; 0.01M, pH = 7.4; Santa Cruz Biotech., CAS30525-89-4) at 4°C for 2-14h. The tissue was then washed extensively with PBS and incubated in streptavidin conjugated to Alexa Fluor 488 (dilution 1:500, ThermoFisher, S32354), Alexa Fluor 555 (1:500, ThermoFisher, S32355) or Alexa Fluor 647 (dilution 1:500, ThermoFisher, S32357) overnight at 4°C. Primary and secondary antibodies were applied as described before (see Experimental procedures, Immunohistochemistry section). After thorough buffer rinses the tissue was mounted on gelatine-coated microscope slides and cover-slipped with anti-fade fluorescent mounting medium (Vectashield Hard Set, VectorLabs; H-1400).

Analysis

Imaging was carried out on a laser scanning confocal microscope (LSM 800, Zeiss) using the 40x objective. For the whole mount preparations, the whole hemisegment of the spinal cord (from lateral side to medial area of the central canal) was scanned generating a z-stack (z-step size = 0.5 – 1 µm). Cell counting was performed in hemisegment 15 of the adult zebrafish spinal cord (in whole mount

preparations). The relative position of the somata of the neurons within the spinal cord, was calculated in whole mount preparations, using the lateral, dorsal, and ventral edges of the spinal cord as well as the central canal as landmarks. The relative position and soma sizes were measured using ImageJ (Schneider et al., 2012, NIH). For better visualization of our data, most of the whole mount images presented here were obtained by merging a subset of the original z-stack, showing the maximal intensity projections for each group. Analysis of the presynaptic terminals was performed of single plane confocal images taken using the 40x oil immerse objective. Colocalizing spots were detected by visual identification of structures whose color reflects the combined contribution of two or more antibodies in the merged image. In addition, analysis of fluorescent intensities for each channel was performed in Imagej software along single lines crossing the structures of interest (intensity spatial profile).
For the *In situ* hybridizations in cryosections (thickness: 25 µm) focal planes with homogeneous and reliable staining for each probe were taken generating a z-stack (z-stack 3-5 µm, z-step size < 1 µm). Only cells with visible $DAPI^+$ nuclei falling within the considered focal planes were examined for the presence of mRNA in the merged images. For the whole mount preparations, larger volumes (30 - 60 µm) of the spinal cord from lateral and from dorsal side ware scanned generating a z-stack (z-step size = 0.5 – 1 µm). As for the cryosections, only small subsets of the original stack (1-4 µm), with homogeneous and reliable staining and $DAPI^+$ nuclei falling within the considered focal planes, were examined for the presence of mRNA in the merged images. All the images were processed in Imagej software.
All figures and graphs were prepared with Adobe Photoshop and Adobe Illustrator (Adobe Systems Inc., San Jose, CA). Digital modifications of the images (brightness and contrast) were minimal so as not to affect the biological information. All double-labeled images were converted to magenta-green immunofluoresence to make this work more accessible to red-green color-blind readers.

Statistics
The significance of differences between the means in experimental groups and conditions was analyzed using parametric tests two-tailed unpaired Student's *t*-test or ordinary *one-way* ANOVA followed by *post hoc* Tukey multiple comparison test, using Prism (GraphPad Software Inc.). Significance levels indicated in all figures are as follows: $*P < 0.05$, $**P < 0.01$, $***P < 0.001$, $****P < 0.0001$. All data are presented as mean ± SEM (Standard error of mean). Finally, the *n* values reflect the final number of validated animals per group or the number of cells that were evaluated.

Supplementary References

Ampatzis, K., and Dermon, C.R. (2010). Regional distribution and cellular localization of beta2-adrenoceptors in the adult zebrafish brain (Danio rerio). J. Comp. Neurol. *518*, 1418–1441.
Ampatzis, K., Kentouri, M., and Dermon, C.R. (2008). Neuronal and glial localization of alpha(2A)-adrenoceptors in the adult zebrafish (Danio rerio) brain. J. Comp. Neurol. *508*, 72–93.
Angulo, M.C., Kozlov, A.S., Charpak, S., and Audinat, E. (2004). Glutamate released from glial cells synchronizes neuronal activity in the hippocampus. Journal of Neuroscience *24*, 6920–6927.
Barreiro-Iglesias, A., Mysiak, K.S., Adrio, F., Rodicio, M.C., Becker, C.G., Becker, T., and Anadón, R. (2013). Distribution of glycinergic neurons in the brain of glycine transporter-2 transgenic Tg(glyt2:Gfp) adult zebrafish: relationship to brain-spinal descending systems. J. Comp. Neurol. *521*, 389–425.
Berg, E.M., Bertuzzi, M., and Ampatzis, K. (2018). Complementary expression of calcium binding proteins delineates the functional organization of the locomotor network. Brain Struct. Funct. *223*, 2181–2196.
Bertuzzi, M., and Ampatzis, K. (2018). Spinal cholinergic interneurons differentially control motoneuron excitability and alter the locomotor network operational range. Sci Rep *8*, 1988.
Bertuzzi, M., Chang, W., and Ampatzis, K. (2018). Adult spinal motoneurons change their neurotransmitter phenotype to control locomotion. Proc. Natl. Acad. Sci. USA *115*, 9926-9933.
Böhm, U.L., Prendergast, A., Djenoune, L., Nunes Figueiredo, S., Gomez, J., Stokes, C., Kaiser, S., Suster, M., Kawakami, K., Charpentier, M., et al. (2016). CSF-contacting neurons regulate locomotion by relaying mechanical stimuli to spinal circuits. Nature Communications *7*, 10866.
Clemente, D., Porteros, Á., Weruaga, E., Alonso, J.R., Arenzana, F.J., Aijón, J., and Arévalo, R. (2004). Cholinergic elements in the zebrafish central nervous system: Histochemical and immunohistochemical analysis. J. Comp. Neurol. *474*, 75–107.

Djenoune, L., Desban, L., Gomez, J., Sternberg, J.R., Prendergast, A., Langui, D., Quan, F.B., Marnas, H., Auer, T.O., Rio, J.-P., et al. (2017). The dual developmental origin of spinal cerebrospinal fluid-contacting neurons gives rise to distinct functional subtypes. Sci Rep *7*, 719.

Hamilton, N.B., and Attwell, D. (2010). Do astrocytes really exocytose neurotransmitters? Nat. Rev. Neurosci. *11*, 227–238.

Higashijima, S.-I., Mandel, G., and Fetcho, J.R. (2004). Distribution of prospective glutamatergic, glycinergic, and GABAergic neurons in embryonic and larval zebrafish. J. Comp. Neurol. *480*, 1–18.

Kuscha, V., Barreiro-Iglesias, A., Becker, C.G., and Becker, T. (2012). Plasticity of tyrosine hydroxylase and serotonergic systems in the regenerating spinal cord of adult zebrafish. J. Comp. Neurol. *520*, 933–951.

McPherson, A.D., Barrios, J.P., Luks-Morgan, S.J., Manfredi, J.P., Bonkowsky, J.L., Douglass, A.D., and Dorsky, R.I. (2016). Motor Behavior Mediated by Continuously Generated Dopaminergic Neurons in the Zebrafish Hypothalamus Recovers after Cell Ablation. Current Biology *26*, 263–269.

Moly, P.K., Ikenaga, T., Kamihagi, C., Islam, A.F.M.T., and Hatta, K. (2014). Identification of initially appearing glycine-immunoreactive neurons in the embryonic zebrafish brain. Dev Neurobiol *74*, 616–632.

Montgomery, J.E., Wiggin, T.D., Rivera-Perez, L.M., Lillesaar, C., and Masino, M.A. (2016). Intraspinal serotonergic neurons consist of two, temporally distinct populations in developing zebrafish. Dev Neurobiol *76*, 673–687.

Mueller, T., Vernier, P., and Wullimann, M.F. (2006). A phylotypic stage in vertebrate brain development: GABA cell patterns in zebrafish compared with mouse. J Comp Neurol *494*, 620–634.

Ohnmacht, J., Yang, Y., Maurer, G.W., Barreiro-Iglesias, A., Tsarouchas, T.M., Wehner, D., Sieger, D., Becker, C.G., and Becker, T. (2016). Spinal motor neurons are regenerated after mechanical lesion and genetic ablation in larval zebrafish. Development *143*, 1464–1474.

Reimer, M.M., Sörensen, I., Kuscha, V., Frank, R.E., Liu, C., Becker, C.G., and Becker, T. (2008). Motor Neuron Regeneration in Adult Zebrafish. J. Neurosci. *28*, 8510–8516.

Rink, E., and Wullimann, M.F. (2004). Connections of the ventral telencephalon (subpallium) in the zebrafish (Danio rerio). Brain Res *1011*, 206–220.

Satou, C., Kimura, Y., Hirata, H., Suster, M.L., Kawakami, K., and Higashijima, S.-I. (2013). Transgenic tools to characterize neuronal properties of discrete populations of zebrafish neurons. Development *140*, 3927–3931.

Schneider, C.A., Rasband, W.S. and Eliceiri, K.W. (2012). NIH Image to ImageJ: 25 years of image analysis. Nature methods *9*, 671-675.